BrO column retrieval algorithms for GOME-2

Ozone SAF visiting scientist
Final Report

April 2007

Nicolas Theys[1], Michel Van Roozendael[1],
Quentin Errera[1], Simon Chabrillat[1], Frank Daerden[1],
François Hendrick[1], Diego Loyola[2], Pieter Valks[2]

[1]Belgian Institute for Space Aeronomy (BIRA-IASB)
3, Avenue Circulaire, B-1180 Brussels, Belgium

[2]DLR-IMF, Oberpfaffenhofen
P.O. Box 1116, D-82230 Wessling, Germany

Summary

The present study is concerned with BrO column retrieval issues in the context of the GOME-2 trace gas operational processor hosted at DLR. Several aspects of the retrieval algorithm are considered. First, DOAS settings optimized for BrO retrieval have been successfully integrated within the UPAS DOAS module at DLR. Further, a series of tests have been conducted in order to validate the radiative transfer tools used for air mass factor calculation, by comparison with the reference DISORT code. Second, a new climatology of stratospheric BrO profiles based on dynamical and chemical indicators has been developed, with the aim to apply it to the retrieval of tropospheric BrO columns from space nadir measurements. The impact of the atmospheric dynamic on the stratospheric BrO distribution is treated by means of Br_y/ozone correlations build from 3D-CTM model results, while photochemical effects are taken into account using stratospheric NO_2 columns as an indicator of the BrO/Br_y ratio. The suitability of the adopted parameterization is evaluated based on one year of output data from the 3D chemistry transport model BASCOE. Model simulations include full gas phase chemistry and relevant heterogeneous reactions, while dynamics is driven by ECMWF wind fields. The approach developed in this work is different from the climatology created by Bruns et al. [2003] in a previous visiting scientist work, in that it aims at representing both the stratospheric BrO profile shape and its integrated column.

Although the suitability of the proposed approach has been demonstrated for most observation conditions, further work is still needed in order to (1) better handle perturbed photochemical conditions during polar spring (ozone hole conditions), and (2) assess the reliability of the BASCOE reference model results by means of validation using ground-based, balloon and satellite observations.

Table of contents

1 Introduction

DLR is responsible within the EUMETSAT O_3 Satellite Application Facility (SAF) for the development of operational products (total ozone columns, NO_2 and BrO columns) of the GOME-2 experiment onboard MetOp. Within this Visiting Scientist project, BIRA-IASB has been supporting DLR with algorithmic developments concerning the retrieval of total and tropospheric BrO columns at the global scale.
In this section, we give an introduction on the role of BrO in the middle atmosphere (stratosphere and troposphere) and we review the main concepts of the retrieval of tropospheric and total BrO columns from space nadir measurements, as developed in Theys et al. (2004). This constitutes a prerequisite to define a practical strategy for the retrieval of tropospheric and total BrO columns for the GOME-2 operational processor hosted at DLR.
In the present report, the following aspects of the retrieval algorithm for GOME-2 will be considered:

- Slant column fitting optimization (section 2)
- Accuracy of radiative transfer tools used for AMF calculation (section 3)
- Development of a stratospheric BrO climatology (section 4)

1.1 BrO in the stratosphere

Inorganic bromine (Br_y=Br, BrO, $BrONO_2$, HBr, HOBr, BrCl) is the second most important halogen that affects stratospheric ozone. Although much less abundant than chlorine, stratospheric bromine presently contributes to the global ozone loss by about 25%, owing to its much larger ozone depletion potential relative to chlorine. The sources of inorganic bromine in the stratosphere are from natural and anthropogenic emitted organic source gases. The major source of organic bromine is methyl bromide (CH_3Br), which is released by natural (oceans) and anthropogenic (e.g. soil fumigation) processes. Additional sources of bromine are the man-made halogenated hydrocarbons gases (halons) initially developed to extinguish fires. Halon-1211 ($CBrClF_2$) and Halon-1301 ($CBrF_3$) are the most abundant halons. Because methyl bromide and the halons are all stable and long-lived, they are transported (principally in the tropical regions) from the ground level to the stratosphere where they are progressively converted into inorganic bromine compounds by direct photolysis or reactions with OH and O. Although the emissions of these long-lived organic bromine species are controlled by the Montreal Protocol since 1987, early signs of a trend stabilization have just been recently identified. The estimate of the stratospheric loading due to long-lived organic bromine compounds is of about 16-17 parts per trillion by volume (pptv). Furthermore, several studies (Pundt et al., 2002; Salawitch et al., 2005; Sioris et al., 2006; Sinnhuber et al., 2002; Sinnhuber et al., 2005; Schofield et al., 2004; Dorf et al., 2006) have suggested a possible additional contribution of 5.6±2 pptv to the total stratospheric inorganic bromine budget by short-lived biogenic organic compounds (such as $CHBr_3$, CH_2Br_2, CH_2BrCl, $CHBr_2Cl$, $CHBrCl_2$ and CH_2BrCH_2Br) or by direct intrusion of tropospheric Br_y into the lower

stratosphere. As a result the ozone loss due to bromine might be underestimated by current models. There is still an intense questioning concerning the evolution of the emissions of short-lived bromine species, in a perspective of a global climate warming (Salawitch, 2006).
Once the organic bromine species are converted in the tropical lower stratosphere into inorganic forms, the bromine compounds experience fast photochemical reactions leading to a partitioning of the various species within the inorganic bromine family (Br_y=Br+BrO+$BrONO_2$+HOBr+HBr+BrCl). The long chemical lifetime of Br_y in the stratosphere allows inorganic bromine to be transported to mid- and high-latitudes, where it affects the stratospheric chemistry.
A brief overview of the stratospheric bromine chemistry according to Lary (1996a) and Lary et al. (1996b) is presented in this section. A complete description of the bromine chemistry has been given in a previous VS activity report (Bruns et al., 2003).
The key bromine photochemical processes in the stratosphere are schematically illustrated in Fig.1.1.

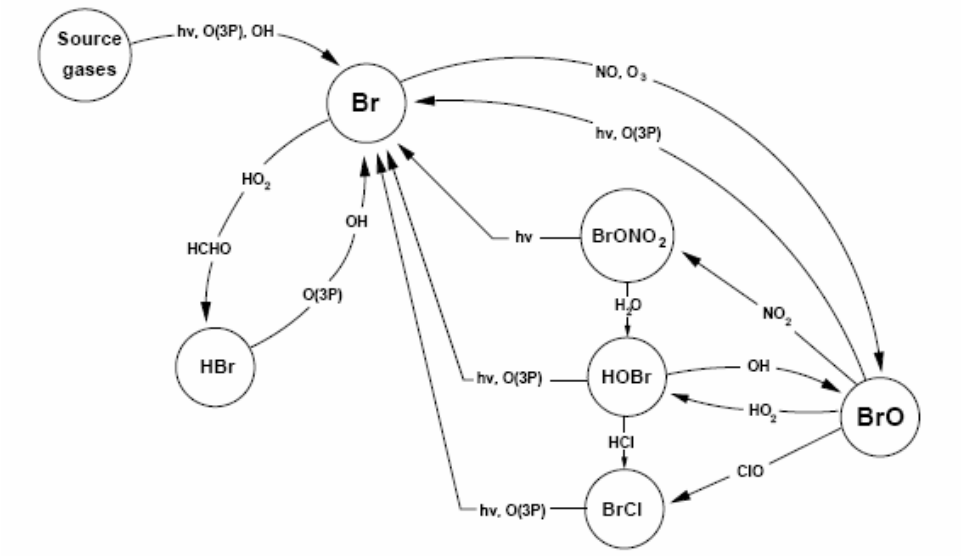

Fig. 1.1: Stratospheric bromine photochemistry scheme. This figure is taken from the PhD. thesis of M. Dorf (2005).

During daytime the most abundant bromine species in the low and middle stratosphere is BrO (40-70% of total Br_y), and is produced by the fast reaction between atomic bromine (Br) and O_3:

$$Br+O_3 \rightarrow BrO+O_2 \qquad \text{(R1)}$$

In usual conditions, the main reactions converting BrO into Br are:

$$BrO+O \rightarrow Br+O_2 \quad \text{(R2)}$$
$$BrO+h\nu \rightarrow Br+O \quad \text{(R3)}$$
$$BrO+NO \rightarrow Br+NO_2 \quad \text{(R4)}$$

The main loss of BrO in the upper stratosphere is due to the reaction with atomic oxygen (R2), while the major destruction mechanisms in the lower stratosphere are provided by photolysis (R3) and the reaction with NO (R4).

During high chlorine activation inside the polar vortex, the dominant reactions which convert BrO into Br are:

$$BrO+ClO \rightarrow Br+OClO \quad \text{(R5a)}$$
$$BrO+ClO \rightarrow Br+ClOO \quad \text{(R5b)}$$

These reactions link two catalytic cycles enhancing the efficiency of both cycles.

The impact of reactive bromine (BrO_x=Br+BrO) on the destruction of ozone is nonetheless moderated by the formation of the bromine reservoirs in reactions with NO_2, HO_2, ClO and HCHO:

$$BrO+NO_2+M \rightarrow BrONO_2+M \quad \text{(R6)}$$
$$BrO+HO_2 \rightarrow HOBr+O_2 \quad \text{(R7)}$$
$$BrO+ClO \rightarrow BrCl+O_2 \quad \text{(R8)}$$
$$Br+HO_2 \rightarrow HBr+O_2 \quad \text{(R9)}$$
$$Br+HCHO \rightarrow HBr+CHO \quad \text{(R10)}$$

Under non-denoxification conditions, bromine nitrate ($BrONO_2$) is the most important bromine reservoir in the stratosphere. HOBr has a lower photolytic stability, and is less abundant during daytime, but is considered as the major night-time reservoir as a result of heterogeneous reactions (see later). HBr accounts to a low fraction of the total Br_y, but is still an important bromine species since HBr is soluble in water and can therefore be removed irreversibly from the stratosphere.
The conversion of bromine reservoirs into reactive bromine is achieved through the following reactions:

$$BrONO_2+h\nu \rightarrow Br+NO_3 \quad \text{(R11a)}$$
$$BrONO_2+h\nu \rightarrow BrO+NO_2 \quad \text{(R11b)}$$
$$HOBr+h\nu \rightarrow Br+OH \quad \text{(R12)}$$
$$HOBr+O \rightarrow BrO+OH \quad \text{(R13)}$$
$$BrCl+h\nu \rightarrow Br+Cl \quad \text{(R14)}$$
$$BrCl+O \rightarrow Br+ClO \quad \text{(R15)}$$
$$HBr+OH \rightarrow Br+H_2O \quad \text{(R16)}$$
$$HBr+O \rightarrow Br+OH \quad \text{(R17)}$$

All these reactions are fast. As a result the partitioning of Br_y is weighted more in the favor of reactive bromine than inactive bromine. This is in contrast with the chlorine chemistry for which, in non-activated conditions, the inorganic chlorine is present in the low and middle stratosphere (below 35 km) essentially as reservoirs (HCl, $ClONO_2$). Thus, bromine is more efficient in destroying ozone than chlorine.
The inorganic bromine species have short chemical lifetime (ranging from ~ 1 s to several minutes) in the sunlit stratosphere, except HBr which has a lifetime close to 1 day in the lower stratosphere. Bromine monoxide (as well as Br, BrONO2, HOBr and BrCl) are hence subject to strong diurnal variations.
Heterogeneous reactions can also affect significantly the bromine chemistry in the stratosphere. The most important reactions are:

$$BrONO_2(g)+H_2O(s) \rightarrow HOBr(g)+HNO_3(s) \quad \text{(R18)}$$
$$BrONO_2(g)+HCl(s) \rightarrow BrCl(g)+HNO_3(s) \quad \text{(R19)}$$
$$HOBr(g)+ HCl(s) \rightarrow BrCl(g)+H_2O(s) \quad \text{(R20)}$$

These reactions are taking place on the surface of aerosols and PSC particles. It is important to note that bromine nitrate can be converted by hydrolysis (R18) on sulfate aerosols into HOBr. At all latitudes and for all seasons, HOBr is the major bromine reservoir before sunrise. Since the photolysis of HOBr is more effective than the photolysis of $BrONO_2$, one expects to observe more BrO in the morning than in the afternoon.
In the polar vortex, bromine species are activated by heterogeneous reactions (R18, R19 and R20) on the surface of PSCs. Inorganic bromine is progressively converted into BrCl during the night. At sunrise, BrCl is photo-dissociated very quickly, leading to a sudden increase of BrO concentrations, higher than usual. During the day, inorganic bromine is almost exclusively partitioned between BrO and BrCl (due to the absence of NO_x by the denoxification process).

The important gas phase and heterogeneous photochemical reactions in the stratosphere, involving inorganic bromine species, are summarized in Table 1.1.

Table 1.1: Stratospheric inorganic bromine photochemistry

Inorganic bromine reactions

Reactive bromine	Reaction Number
$Br+O_3 \rightarrow BrO+O_2$	R1
$BrO+O \rightarrow Br+O_2$	R2
$BrO+h\nu \rightarrow Br+O \quad (\lambda \leq 515nm)$	R3
$BrO+NO \rightarrow Br+NO2$	R4
$BrO+ClO \rightarrow Br+OClO \quad (59\%)$	R5a
$Br+ClOO \quad (34\%)$	R5b

Conversion of bromine reservoirs	Reaction Number
$BrONO_2+h\nu \rightarrow Br+NO_3 \quad (\lambda \leq 861nm)$	R11a
$\rightarrow BrO+NO_2 \quad (\lambda \leq 1129nm)$	R11b
$HOBr+h\nu \rightarrow Br+OH \quad (\lambda \leq 578nm)$	R12
$HOBr+O \rightarrow BrO+OH$	R13
$BrCl+h\nu \rightarrow Br+Cl \quad (\lambda \leq 546nm)$	R14
$BrCl+O \rightarrow Br+ClO$	R15
$HBr+OH \rightarrow Br+H_2O$	R16
$HBr+O \rightarrow Br+OH$	R17

Formation of bromine reservoirs	
$BrO+NO_2+M \rightarrow BrONO_2+M$	R6
$BrO+HO_2 \rightarrow HOBr+O_2$	R7
$BrO+ClO \rightarrow BrCl+O_2 \quad (7\%)$	R8
$Br+HO_2 \rightarrow HBr+O_2$	R9
$Br+HCHO \rightarrow HBr+CHO$	R10

Heterogeneous bromine reactions	
$BrONO_2(g)+H_2O(s) \rightarrow HOBr(g)+HNO_3(s)$	R18
$BrONO_2(g)+HCl(s) \rightarrow BrCl(g)+HNO_3(s)$	R19
$HOBr(g)+HCl(s) \rightarrow BrCl(g)+H_2O(s)$	R20

1.2 BrO in the troposphere

Stratospheric and tropospheric bromine chemistry differs in major ways. The UV flux necessary for the photolysis of the inorganic bromine precursors is lower in the troposphere than in the stratosphere. Furthermore, the soluble bromine organic compounds are removed efficiently from the atmosphere by wet deposition. Finally, the fundamentally different structure and composition of the troposphere compared to the stratosphere strongly affect the chemistry of bromine species in the troposphere.
Nevertheless, during the last decade, it was found that bromine species can be present in the troposphere as inorganic compounds. BrO has been found massively in the planetary boundary layer during polar tropospheric ozone depletion events (Hausmann and Platt, 1994; Kreher et al., 1997; Hönninger and Platt, 2002; Frieβ et al., 2004). The sudden increase in BrO (the so-called "bromine explosion" phenomenon), is observed every year in both polar regions at spring (Wagner et al., 1998; Richter et al., 1998; Wagner et al., 2001) and is responsible for complete removal of the ozone within hours or days. The exact mechanism for the release of bromine is currently not fully understood. The autocatalytic release from sea salt by heterogeneous reactions has been proposed. There is evidence for the involvement of frost flowers (Kaleschke et al., 2004). BrO has also

been identified over salt lakes (Hebestreit et al., 1999), in the marine boundary layer (Leser et al., 2003) and in volcanic plumes (Bobrowski et al., 2003).
Futhermore, satellite observations have found strong indications for the widespread presence of BrO in the free troposphere with vertical columns of about 1-3 x 10^{13} molec/cm^2 (Wagner and Platt, 1998; Pundt et al., 2000; Van Roozendael et al., 2002; Richter et al., 2002a), probably due to the decomposition of short-lived organic bromine compounds by heterogeneous or gas-phase photochemistry. Recent modeling results (von Glasow et al., 2004) have shown that this may represent a significant sink for O_3 that has been so far ignored in most tropospheric chemistry studies and models. It could lead to a reduction in the zonal mean O_3 mixing ratio of up to 18% and locally even up to 40% compared to a scenario without bromine chemistry. The assumed concentration of BrO in the free troposphere can lead to several important effects on the tropospheric chemistry. It can affect the oxidizing capacity of the troposphere through its effect on ozone concentration. In addition, it changes the partitioning NO_2/NO and HO_2/OH, but can also release reactive chlorine species.

1.3 BrO retrieval from space nadir measurements

The aim for the off-line operational GOME-2 BrO product will be to derive accurate tropospheric and total BrO columns. In order to reach these goals, total BrO columns must be resolved into their stratospheric and tropospheric contributions. From the measurements alone, there is no way to separate the two components. Further, the approach used for the retrieval of tropospheric NO_2 columns based on a reference sector method (Richter et al., 2002b) cannot be applied for BrO because of the longitudinal inhomogeneity of stratospheric BrO and the difficulty to find an area without any tropospheric contamination. An algorithm to retrieve tropospheric BrO columns from GOME measurements has been developed at BIRA-IASB. This method is based on a residual approach (Theys et al., 2004), where the stratospheric BrO contribution is determined from the 3D chemical transport model (CTM) SLIMCAT (Chipperfield et al., 2002), and is then subtracted from the measured total BrO colum to provide the tropospheric BrO column. Such a complex approach is not applicable in an operational context and simplifications have to be found and applied. In this section, the important aspects of this scientific algorithm are presented. They will serve as reference in this study, in order to define a retrieval strategy applicable for GOME-2 operational retrieval of BrO within the existing UPAS environment.

As a first step, the BrO slant column densities (SCD) from GOME were inverted by applying the DOAS method on the 344.7-359 spectral range. The settings basically follow the recommendations issued in the extensive study of Aliwell et al. (2002). The BrO absorption cross-sections used are those from Wilmouth et al. (1999), convolved to the GOME resolution, which is derived as part of the retrieval algorithm. The DOAS procedure accounts for the GOME undersampling (Chance, 1998). More details on the DOAS procedure applied can be found in section 2 and in Van Roozendael et al. (1999).

The tropospheric algorithm is based on a residual method. The tropospheric contribution is obtained by substracting a stratospheric slant column from the total slant column densities. The stratospheric BrO correction is derived from estimates of the stratospheric vertical column multiplied by an appropriate air mass factor (AMF). Finally, tropospheric AMFs are applied to residual tropospheric SCDs to give tropospheric vertical column densities. The overall structure of the algorithm is outlined on Fig. 1.2.

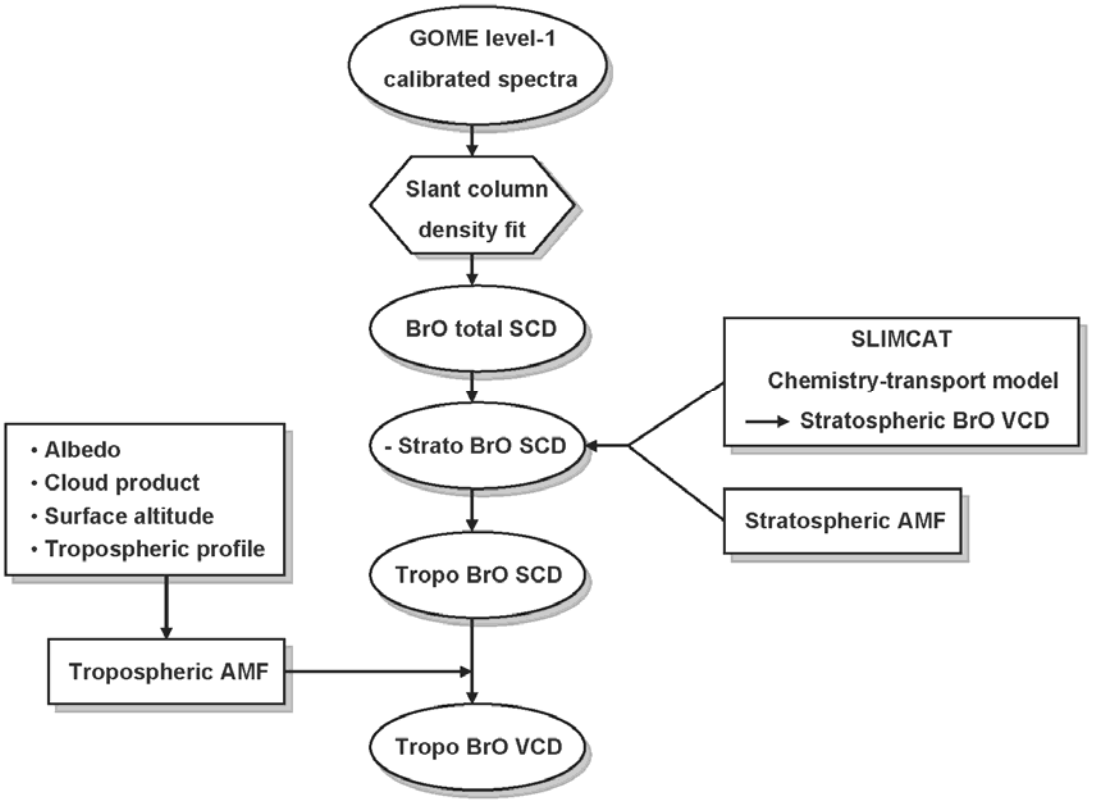

Fig.1.2: Overview of the tropospheric BrO retrieval algorithm

The approach followed in Theys et al. (2004) was to use the 3D-CTM SLIMCAT model as a stratospheric reference. Modeled stratospheric BrO profiles are integrated from the tropopause (determined from ECMWF data (Reichler et al., 2003)) to the top-of-atmosphere.
To convert SCD to vertical columns (VCD), the computation of an air mass factor is needed:

$$VCD = \frac{SCD}{AMF} \tag{1.1}$$

The stratospheric AMF is in general very different than the tropospheric AMF, illustrating the difference in measurement sensitivity at the two altitude levels. It has been proven that for thin absorbers (as BrO), the AMF depends on the profile linearly (Palmer et al., 2001):

$$AMF = \int w(z) Prof(z) dz \qquad (1.2)$$

where $Prof(z)$ is the normalized atmospheric profile and $w(z)$ is the so-called weighting function (expressed in cm). One of the most important issue is to apply this formula to consistent profiles. The weighting function (WF) represents the sensitivity of the measurement at a certain altitude and can be interpret as a height-resolved air mass factor. The weighting function contains all the dependences (except the atmospheric profile) to:

- Solar zenith angle
- Viewing angle
- Relative azimuth angle
- Surface altitude
- Surface albedo
- Cloud top height
- Cloud fraction

Look-up-tables of scattering weighting functions have been calculated for gridded values of these parameters (at 352 nm, a wavelength assumed to be representative of the BrO fitting window) with the radiative transfer model UVspec/DISORT package (Mayer and Killing, 2005).

Impact of surface albedo

As an example, Fig. 1.3 presents height-resolved air mass factors for BrO assuming low (6%) and high (80%) surface albedo respectively.

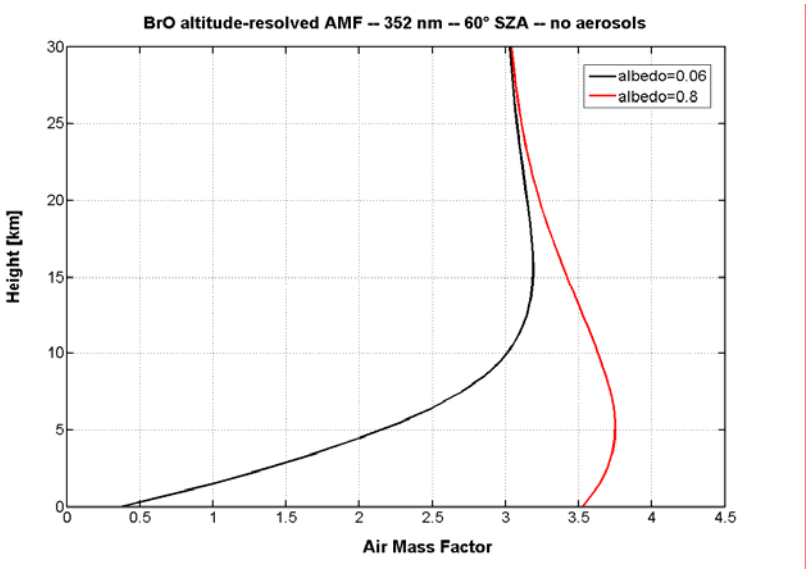

Fig. 1.3: Altitude-resolved AMF for BrO space nadir measurements assuming a solar zenith angle of 60°, no aerosols, at a wavelength of 352 nm, for typical low (6%) and high (80%) surface albedos.

The influence of ground albedo on the sensitivity of the satellite observations to tropospheric species is strong compared to the stratosphere. The sensitivity to boundary layer is large when the ground albedo is high. The case of high ground albedo is optimal for tropospheric observations since the sensitivity is maximum and the weighting functions are weakly dependent on the altitude.
As the tropospheric AMF is very sensitive to the surface albedo, the monthly database at 335 nm from (Koelemeijer) is used.

Impact of clouds

In first approximation, clouds can be seen as highly reflecting surfaces. If the cloud lies under a BrO layer, BrO measurements are expected to be enhanced by its reflectivity. On the opposite, if the cloud lies above the BrO layer, it will hide BrO from measurements. In principle this effect can be accounted for through the use of a ghost column correction, if it is known.
To account for the effect of the clouds, we use the output of the FRESCO algorithm. FRESCO simultaneously retrieves the effective cloud fraction and cloud top pressure from GOME data (Koelemeijer et al., 2001). This algorithm makes use of reflectivities as measured by GOME inside and outside the oxygen A band (758-778 nm). Cloud fractions and cloud top pressure from FRESCO are used to weight the AMFs for partly cloudy pixels (independent pixel approximation).

BrO vertical profile

In order to derive accurate BrO AMFs, scattering weighting functions have to be applied to realistic BrO profiles. This is especially important in the troposphere since at altitudes below 10 km, the scattering weights are strongly dependent on the altitude (see Fig. 1.3). Given the current lack of knowledge about the behaviour of BrO content in the troposphere, we have assumed the tropospheric BrO profile to have a main free-tropospheric contribution: a gaussian profile with a maximum at 6 km high and a full width half maximum of 2 km has been chosen. This choice is consistent with tropospheric BrO measurement reported in the literature (Fitzenberg et al., 2000; Theys et al., 2007). However, a special case has been designed for polar regions with high albedo (snow-ice cover): if the retrieved tropospheric vertical column exceeds a certain threshold (arbitrary fixed at 6.5e13 molec/cm²) we assume it is because of emissions at the surface level. In this case a different tropospheric profile is introduced: constant in the first 2 km from the altitude of the reflector retrieved by FRESCO. This simulates the “bromine explosion” phenomenon in polar regions in spring. The net effect of this dynamical adjustment of the BrO profile is to increase the size of BrO emissions for polar regions.

Using our residual analysis scheme based on the SLIMCAT model data, tropospheric BrO VCDs have been computed for all GOME measurements. The monthly mean for September 1997 in the southern hemisphere is displayed in Fig. 1.4, as an illustration of the results. The bromine emissions at the surface in polar regions in spring are clearly visible. The high tropospheric BrO columns are located on areas around the Antarctica continent, where the potential of frost flower coverage is high.

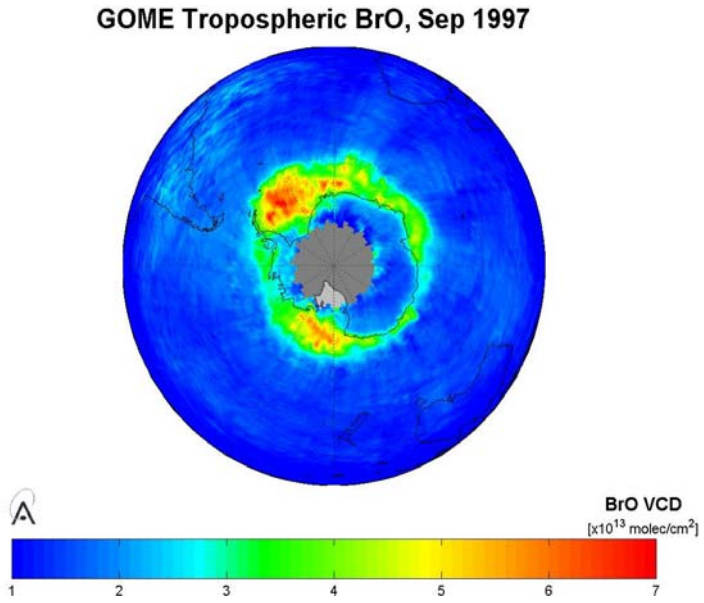

Fig. 1.4: Monthly averaged tropospheric BrO vertical columns over the southern hemisphere derived from GOME observations, for September 1997.

Once the tropospheric BrO vertical column has been retrieved, the total BrO VCD can be calculated simply by dividing the measured SCD by a total AMF:

$$AMF_{total} = \frac{AMF_{tropo} VCD_{tropo} + AMF_{strato} VCD_{strato}}{VCD_{tropo} + VCD_{strato}} \tag{1.3}$$

which is necessary to correct for the difference of measurement sensitivity at the stratosphere and the troposphere. These total vertical columns constitute an improvement of the vertical columns provided by using quasi geometric AMFs adequate only for a stratospheric absorber.

2 DOAS BrO retrieval

The BrO slant column densities from GOME/ERS-2 were inverted by applying the DOAS method on the 344.7-359 spectral range, making use of the characteristic absorption structures of BrO in this region. The settings follow the recommendations of Aliwell et al. (2002). The BrO absorption cross-sections used (Wilmouth et al., 1999) are convolved to the GOME resolution, which is derived as part of the retrieval algorithm. The DOAS procedure accounts for the GOME undersampling (Chance, 1998). For GOME, the BrO DOAS settings are summarized in Table 2.1 (details can be found in Van Roozendael et al., 1999).

Table 2.1 : Analysis settings used for GOME BrO slant column fitting.

Fitting interval :	344.7-359 nm
Molecular absorption cross-sections :	
BrO	228°K [Wilmouth et al., 1999]
O_3	221°K, 241°K [Burrows et al., 1999]
NO_2	221°K [Burrows et al., 1998]
O_4	[Greenblatt et al., 1990]
OClO	[Kromminga et al., 1999]
H_2CO	[Cantrell et al., 1990]
Additional features :	
Closure polynomial	order 3
Ring treatment	Cross-section calculated using SCIATRAN model [Vountas et al., 1998]
Undersampling	[Chance, 1998]
Offset correction	Slope (2 parameters)
Shift of O_3 and NO_2 cross-sections	0.03 nm
Wavelength calibration	Based on Kurucz solar spectrum

In the framework of this Visiting Scientist project, the BrO DOAS algorithm of the operational UPAS system at DLR has been synchronized with the BIRA WinDOAS code, using the DOAS settings described in Table 2.1. Consistency has been checked on sample orbits from GOME/ERS-2 under various conditions of BrO loading and latitude/season. We find a good agreement with differences smaller than 2% (see Figure 2.1).

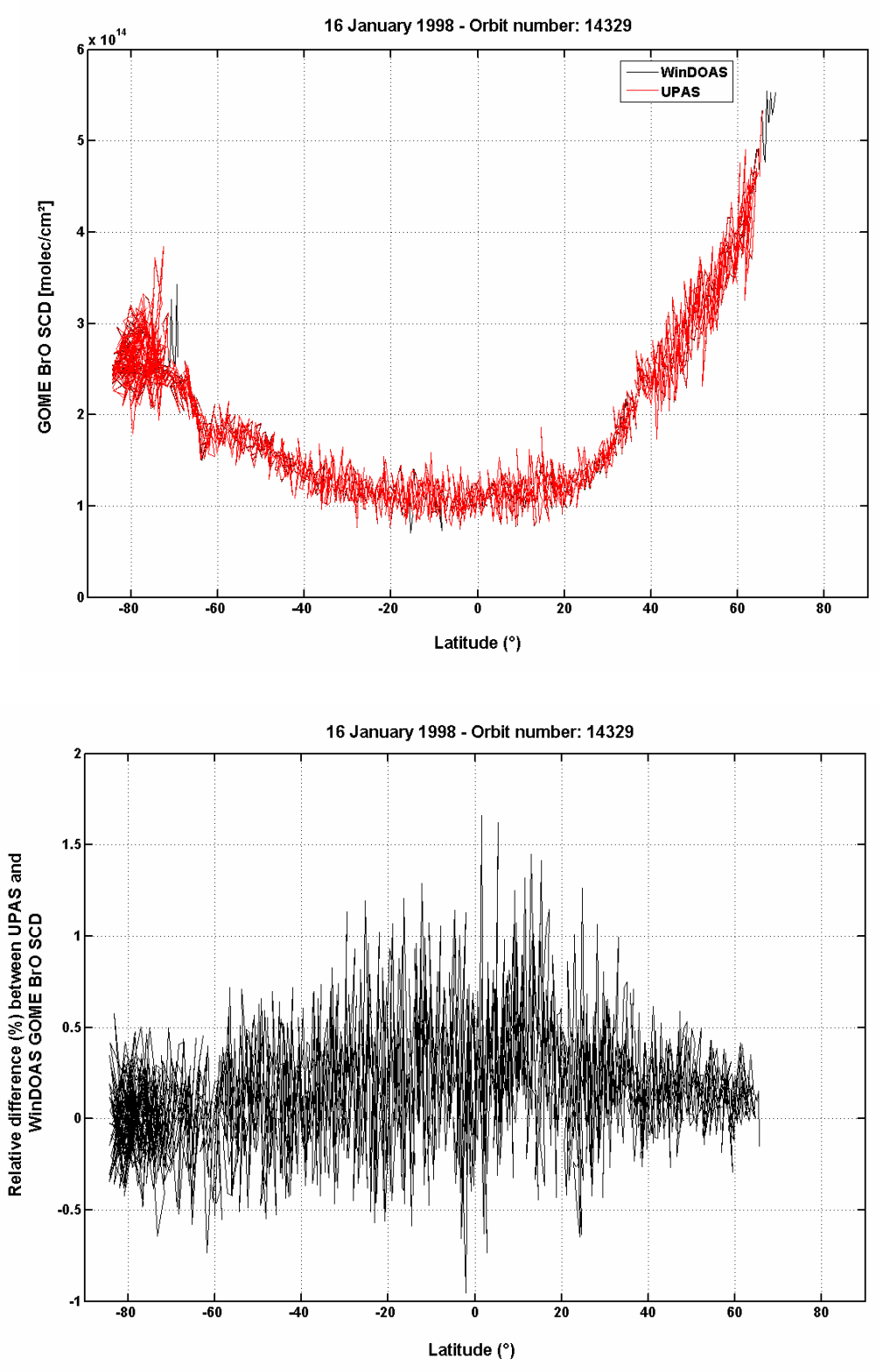

Fig. 2.1: Comparison of BrO slant columns retrieved from GOME/ERS-2 using the UPAS system and the WinDOAS code, for the orbit 14329. The lower plot corresponds to the relative difference between UPAS and WinDOAS BrO SCDs

For GOME-2/MetOp, the baseline BrO slant column retrieval is very similar to that for GOME/ERS-2. The same BrO fitting interval is foreseen for GOME-2. The BrO absorption cross-sections from Wilmouth et al. [1999] will be convolved with the GOME-2 slit-function [Siddans et al., 2006]. The same applies to the absorption cross-sections of O_4, OClO and HCHO. For O_3 and NO_2, the CATGAS GOME-2 FM absorption cross-sections can be used [Gür et al., 2005]. A Ring cross-section for GOME-2 has been provided by Van Roozendael [Pers. Comm. 2006]. The inclusion of an undersampling correction is probably not needed for the GOME-2 instrument.

3 Accuracy of radiative transfer tools for AMF calculation

We present the results of an intercomparison exercise between two different radiative transfer (RT) models carried out in the framework of the Ozone SAF Visiting Scientist project. The RT models involved are the LIDORT v2.2+ model and the UVspec/DISORT package. A summary of the characteristics of the models is given in Table 3.1.

Table 3.1: Short description of the RT models involved in the intercomparison exercise.

Name	Model main features	Reference
LIDORT v2.2+	- Multi layer multiple scatter discrete ordinate model - spherical-shell treatment for dealing with wide off-nadir viewing	Spurr et al., 2001 Spurr 2003
UVspec/DISORT package	- Discrete ordinate method - Treatment of MS and refraction in a pseudo-spherical geometry (direct beam only) - Treatments for aerosol and cloud scattering, and ground albedo	Mayer and Kylling (2005)

Box-air-mass-factors (box-AMFs) of BrO and NO2 for various atmospheric height layers were modeled and compared. The box-AMF is defined here, as the ratio of the partial SCD to the partial VCD of an atmospheric layer with a constant trace gas optical depth:

$$AMF_i = \frac{SCD_i}{VCD_i} \tag{3.1}$$

The box-AMFs describe the sensitivity of the measurements as a function of the altitude and can be used easily to calculate the total AMFs using a given trace-gas profile:

$$AMF = \frac{\sum_{i=1}^{n_{layers}} AMF_i \,.\, VCD_i}{\sum_{i=1}^{n_{layers}} VCD_i} \qquad (3.2)$$

Equation (3.2) is the discrete equivalent of equation (1.2). Accurate box-AMFs are of great importance for the retrieval of vertical columns of trace gases from satellite nadir measurements. This is particularly the case for the retrieval of tropospheric and total BrO and NO2 columns, as explained in section 1.3.
The box-AMFs can be computed in a similar procedure as total AMFs. Instead of inserting a vertical profile in the RT code, an absorber is inserted at one layer and no absorbers in the other layers. The calculation is then repeated for a number of layers. For this purpose, we used 24 layers defined by the following layer boundaries pressure (expressed in mb): 1050, 1041.88, 1021.63, 983, 924.78, 848.92, 759.68, 662.18, 561.89, 463.86, 372.42, 290.82, 221.17, 164.28, 119.82, 86.18, 60.18, 39.58, 25.8, 16.8, 10.96, 7.12, 4.66, 2.98, 0.03. These pressures are based on the 35 level ECMWF hybrid level definition.
The box-AMFs have been calculated with most settings common for both models, as summarized in Table 3.2.

Table 3.2: Model settings for the box-AMFs comparison

Geometry	pseudo-spherical (DISORT) spherical-shell treatment (LIDORT)
Number of streams	8 (LIDORT); (10: DISORT)
Scattering mode	multiple scattering
Rayleigh scattering	included
Mie scattering	not included
Refraction	not included
Temperature profile	Mid-Latitude Summer profiles of the US standard atmosphere
Lambertian surface reflection	

The calculation of the box-AMFs have been performed at 352 and 439 nm, representative for the fitting windows of BrO and NO_2, respectively. The box-AMFs calculation are made by introducing a trace gas amount of fixed optical thickness in each layer: 0.0001 for BrO and 0.002 for NO_2.
A number of plausible atmospheric scenarios have been chosen for the AMFs comparison. Box-AMFs have been generated with both RT models by varying the solar zenith angle μ_o=cos(sza), the viewing zenith angle μ=cos(vza), the relative azimuth angle φ, the surface albedo a_s and the surface pressure p_s, see Table 3.3.

Table 3.3: Geometry and surface parameter values for the Box-AMFs comparison

Parameters	**Values**
μ_o	0.90 0.50 0.15 (*sza=25.8°, 60°, 81.4°)*
μ	1.00 0.70 (*vza=0°, 45.6°)*
φ	0 100 180
a_s	0.025 0.15 0.8
p_s	1021.63 561.89

The box-AMFs from the two models have been compared and the differences between the two RT model results were systematically investigated with respect to their dependence on the solar zenith angle, viewing zenith angle, relative azimuth angle, albedo and surface pressure.
Fig. 3.1 shows examples of the comparisons of the Box-AMFs between DISORT and LIDORT for different scenarios.

(a) (b)

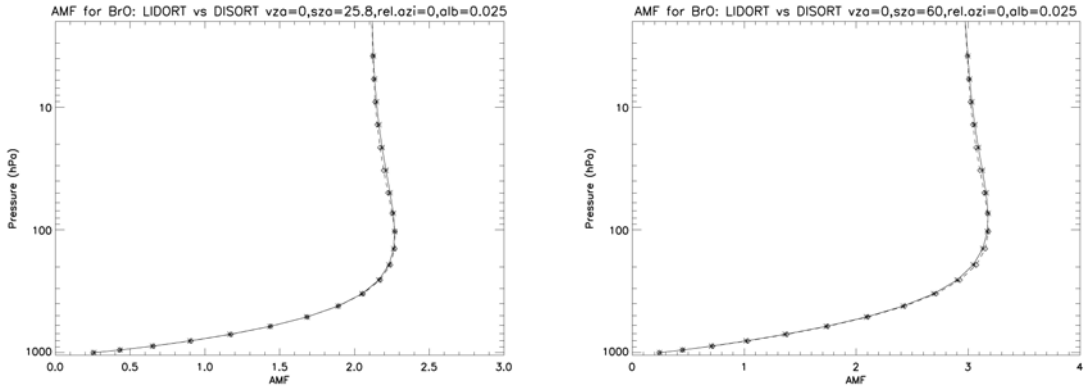

(c) (d)

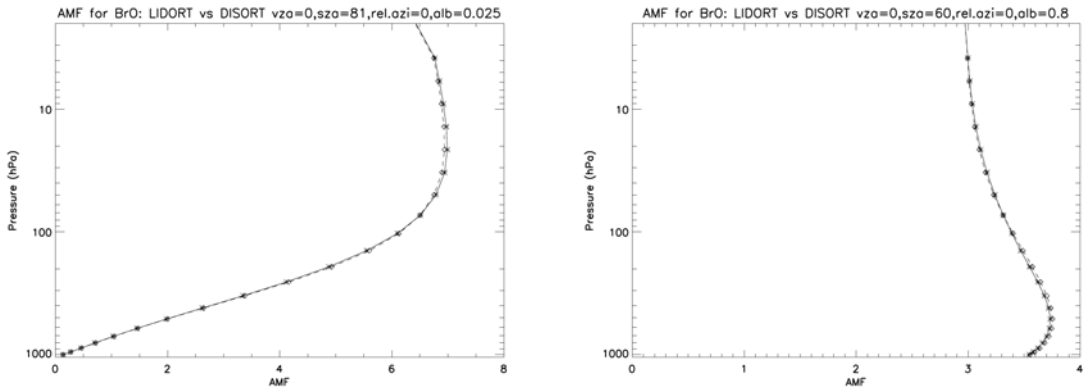

(e)

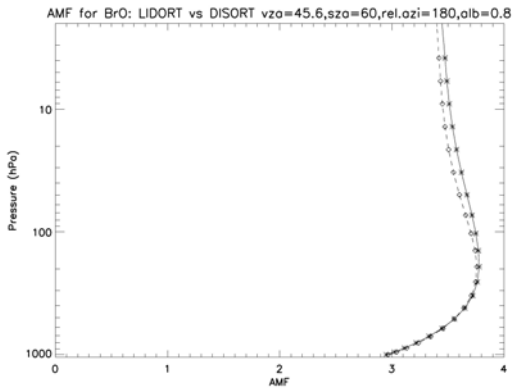

(f)

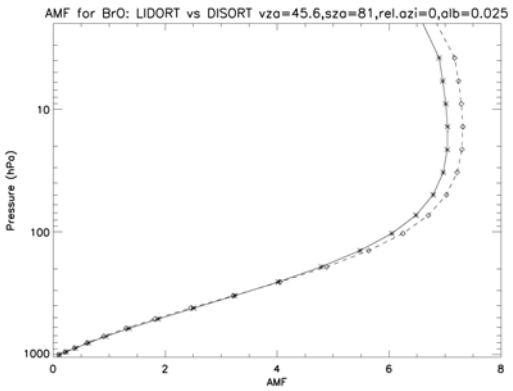

(g)

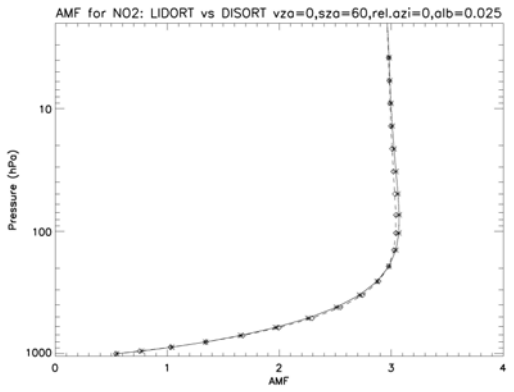

Fig. 3.1: Box-AMFs comparisons between DISORT (squares) and LIDORT (stars) for:
(a) BrO, sza=25.8°, vza=0°, φ=0°, a_s=0.025
(b) BrO, sza=60.0°, vza=0°, φ=0°, a_s=0.025
(c) BrO, sza=81.0°, vza=0°, φ=0°, a_s=0.025
(d) BrO, sza=60.0°, vza=0°, φ=0°, a_s=0.80
(e) BrO, sza=60.0°, vza=45.6°, φ=180°, a_s=0.80
(f) BrO, sza=81.0°, vza=45.6°, φ=0°, a_s=0.025
(g) NO_2, sza=60.0°, vza=0°, φ=0°, a_s=0.025

(surface pressure=1021.63 hPa)

The DISORT and LIDORT Box-AMFs are in good agreement for both wavelengths (BrO and NO_2 AMFs). The agreement is within 1-2%, except for high VZA at high SZA where the differences are of about 5%. These discrepancies are due to the treatment of the Earth's sphericity, which is different in both models. DISORT uses the classical pseudo-spherical approximation, which means that sphericity is only taken into account for the calculation of the attenuated incident beam, while the multiple scattering term is treated in a plane-parallel atmosphere. In contrast to LIDORT, there is no further correction to account for the sphericity along the line-of-sight. This results in larger errors in the DISORT Box-AMF for large line-of-sight angles, especially at high solar zenith angles.

4 A stratospheric BrO climatology based on the BASCOE model

As explained in section 1.3, the calculation of a stratospheric correction (i.e. a stratospheric BrO slant column) is necessary for the retrieval of tropospheric and (improved) total columns. During the present Visiting Scientist work, a stratospheric BrO column and profile climatology based on BASCOE model results has been developed, for use in the operational processing of tropospheric and total BrO columns from GOME-2 measurements. This study is complementary to the previous Visiting Scientist work of Bruns et al. (2003) which was dedicated to the creation of a climatological data base of BrO profiles for air mass factors calculation.

4.1 The BASCOE model

The Belgian Assimilation System of Chemical Observations from ENVISAT (BASCOE[1]) is a 4D-Var assimilation system designed for the analysis and forecast of stratospheric ozone and chemical fields (Errera and Fonteyn, 2001). The model includes 57 chemical species and 4 types of stratospheric PSC particles (ice; supercooled ternary solution, STS; nitric acid trihydrate, NAT; sulphuric acid tetrahydate, SAT) with a full description of stratospheric chemistry and microphysics of PSCs. All chemical species are advected and interact through 143 gas-phase reactions, 48 photolysis reactions and 9 heterogeneous reactions, all listed in the latest Jet Propulsion Laboratory compilation (Sander et al., 2003). PSC microphysics is described by the PSCBox scheme (Larsen et al., 2000) which is coupled to the 3D-CTM core model.
The data used in the present study results from a free model run, with a model version referred to as v3f98. It is very similar to the one described in Daerden et al. (2006). The simulations start on 1 May 2003 and end on 30 April 2004, covering one year of data. The horizontal resolution is of 1.875° in latitude and 2.5° in longitude. The model is defined on 37 vertical levels, from the surface to 0.1 hPa. It is driven by the ECMWF operational forecasts of winds and temperatures. The integration time step is 15 min. The model chemical fields are initialized from an output of the SLIMCAT chemical model interpolated to the BASCOE grid. The BASCOE output consist of hdf daily files containing the volume mixing ratios of the chemical species at 00:00, 06:00, 12:00, 18:00 and 24:00 universal time.

In an attempt to assess the reliability of the BASCOE system, several studies have been conducted recently, leading to the general conclusion that BASCOE provides acceptable results, which are consistent with the available observational data sets. More information can be found in the following recent publications:

- Daerden et al., 2006: Simulations are presented for the Antarctic winter of 2003 and comparisons are made to a set of MIPAS (N_2O, HNO_3, H_2O and O_3 profiles) and

[1] http://www.bascoe.oma.be

POAM III (aerosol and PSC extinction, H_2O and O_3 profiles) observations. This study shows that BASCOE is able to reproduce well processes such as tracer evolution, denitrification, dehydration and ozone depletion.

- Geer et al., 2006: It examines 11 sets of ozone analysis from 7 different Data Assimilation systems (including BASCOE). This intercomparison exercise includes observational data sets from MIPAS, HALOE and ozone sondes. BASCOE gives good results and is, in general, in line with the other Data Assimilation systems.
- Vigouroux et al., 2007: deals with comparisons between ground-based FTIR and MIPAS N_2O and HNO_3 profiles assimilated in the BASCOE system. It shows good agreement between MIPAS and FTIR observations.

4.2 General approach

The stratospheric BrO climatology developed here, has to meet specific requirements to be suitable for tropospheric BrO columns retrieval. Since the orbits of the MetOp platforms (carrying the GOME-2 experiment instruments) are quasi polar, the coverage is nearly global, so the climatology has to cover all latitudes from pole-to-pole. Furthermore it is required to take into account the diurnal variation of BrO, as the instrument is sounding the atmosphere for a large range of possible solar zenith angles. However, at large SZA, BrO SCDs retrieved from space nadir measurements are almost exclusively dominated by the absorption in the stratosphere. Indeed, the very large photon paths in the stratosphere coincide with a decreased sensitivity to the troposphere. Thus, it is recommended to consider in the tropospheric BrO column retrieval only the measurements corresponding to SZA lower than 85°, in order to avoid unrealistic results.
Furthermore, at high solar zenith angle, a scenario where BrO has a strong variation within the measured pixel due to inhomogeneous SZA, can not be avoided.
Stratospheric BrO is highly variable in time and space, and depends of several parameters and atmospheric conditions. The BrO climatology proposed here, to be adequate for the present application, must be able to reproduce accurately the BrO profiles for the large variety of possible scenarios. Fig. 4.1 represents the stratospheric BrO vertical columns as derived from the SLIMCAT model for the 15 March 2000, at the time of GOME overpass (around one hour later than GOME-2 overpass).

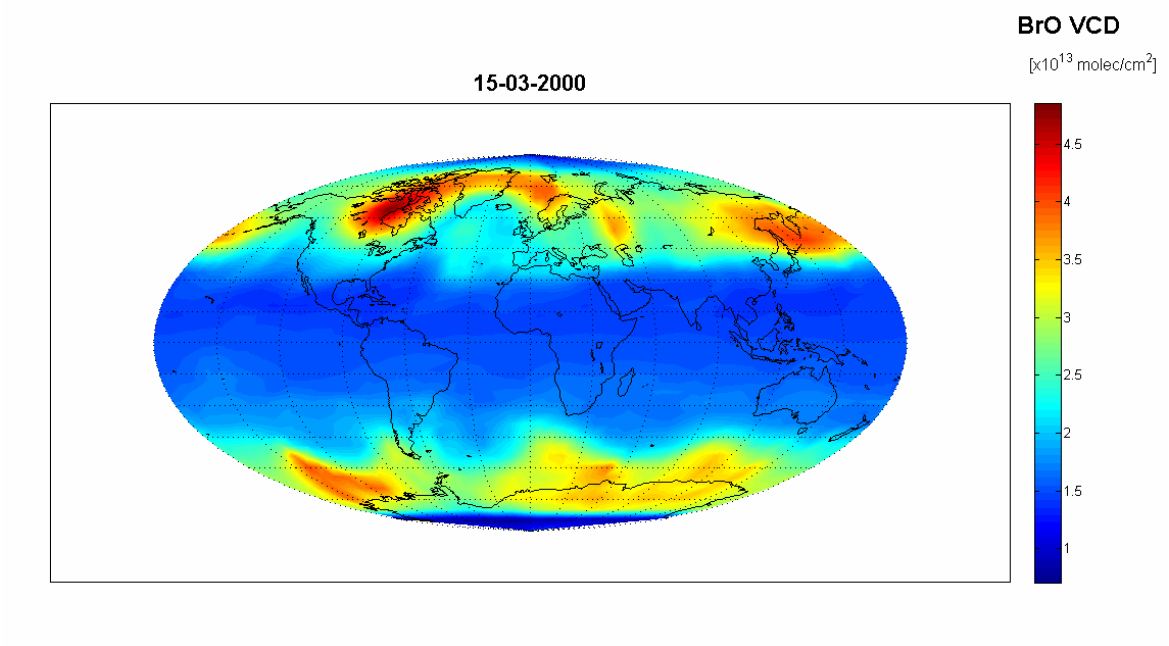

Fig. 4.1: Example of SLIMCAT stratospheric BrO vertical columns at the time of GOME overpass.

This map illustrates the high variability of BrO in the stratosphere at mid- and high latitudes. The large structures shown here, reflect the strong effect of atmospheric dynamic on the BrO distribution. It can be deduced from Fig. 4.1 that adopting a zonal mean climatology approach (as in Bruns et al., 2003) will often lead to errors on the mid- and high latitude stratospheric columns of about 0.5 $x10^{13}$ molec/cm^2, due to the longitudinal inhomogeneity of BrO . The amplification of this error by a factor AMF_{strato}/AMF_{tropo} (sometimes higher than 4!) will lead to unacceptable artifacts in the tropospheric column product. Fig. 4.1 shows in particular that it will be the case in high latitude regions for periods when large BrO emissions in the boundary layer are known to occur.

Our climatology would have to reproduce qualitatively and quantitatively the general patterns of stratospheric BrO. What we need here, is to establish a (simple or sophisticated) parameterization of the stratospheric BrO profiles which takes into account somehow the main processes controlling the distribution of BrO in the stratosphere.

BrO in the stratosphere is affecting by both the dynamic of the atmosphere and the photochemistry.

The bromine monoxide volume mixing ratio profile can be written:

$$BrO = Br_y \times \frac{BrO}{Br_y} \qquad (4.1)$$

where $Br_y = Br + BrO + BrONO_2 + HOBr + HBr + BrCl + 2Br_2$ is the inorganic bromine profile accounting for all inorganic bromine species (active bromine and bromine reservoirs). Br_y, considered as an atmospheric species, has a very long chemical life time (several years or decades). Thus, a given air parcel in the stratosphere will be transported, maintaining its initial Br_y volume mixing ratio. Br_y (and other species like N_2O or CH_4) can be considered as a good chemical tracer of the dynamic of the atmosphere. Within the

given air parcel, rapid photochemical reactions between the various inorganic bromine species are taking place and affect the partitioning of BrO into the inorganic bromine species family (BrO/Br_y). In summary, equation (4.1) separates the effects on the BrO vertical distribution due to the dynamic of the atmosphere (affecting Br_y) and the photochemistry (affecting BrO/Br_y). In this study, we decided to treat these two different aspects separately by developing two distinguished "climatologies". The development of a Br_y profile climatology is the focus of section 4.2.1, while a "partitioning" profile climatology (BrO/Br_y) is presented in section 4.2.2.
In practice, the key aspect to derive a suitable stratospheric BrO profile is to obtain sufficiently information about the dynamical and photochemical state of the sounded atmosphere. The approach adopted in the present study, and which will be developed in the next sections, is that we can reach this goal by using a limited number of geophysical parameters, in addition to the geolocation information (date & time of the measurement, center coordinate of the ground pixel and solar zenith angle). Moreover, it will be demonstrated that the use of some of the operational level-2 products of GOME-2 (Total ozone column, ozone profile, NO_2 columns,…) is of great help to determine a trustworthy stratospheric BrO profile representative of the measured pixels.

4.2.1 Dynamic of the stratosphere

As a first approximation, it can be assumed that air parcels in the lower stratosphere are transported adiabatically. This hypothesis seems plausible for atmospheric motion as advection with typical timescale of ~ 1 day. Several dynamical variables (as potential temperature and potential vorticity) are conserved during adiabatic motions. As Br_y has a very long chemical lifetime and if we assume that the sources of Br_y are stable, these variables might be used to evaluate air parcel trajectories and, at the end, to reconstruct reliable Br_y profiles. Nevertheless, this approach is relatively inconvenient to implement for operational processing, since it needs external meteorological data. Indeed, the potential temperature and the potential vorticity are calculated by using temperature profiles and wind fields (the gradient of the wind vector, to be precise).
However, a simpler approach can be adopted which use the O_3 column as a good indicator of the dynamic of the atmosphere.

Before entering into the details, it is interesting to make a qualitative comparison between the BrO VCD presented in Fig. 4.1 and the O_3 VCD corresponding to the same date shown in Fig. 4.2.

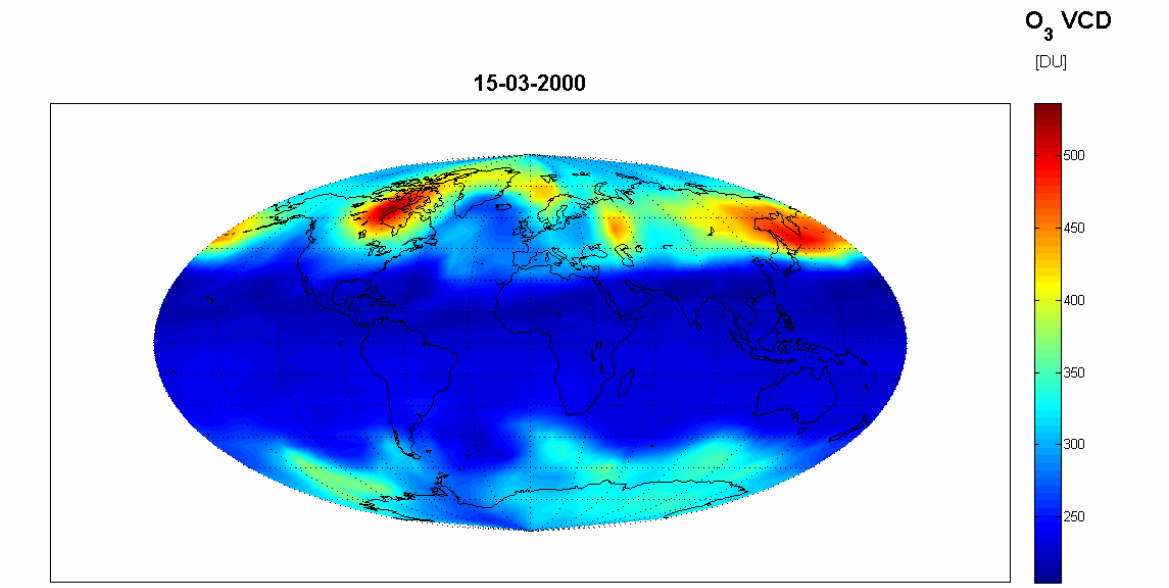

Fig. 4.2: Example of SLIMCAT O_3 vertical columns at the time of GOME overpass, corresponding to the same date than the BrO vertical columns shown in Fig. 4.1.

A strong correlation between the BrO VCD and the O_3 VCD appears almost everywhere, except at very high latitudes (in other words at high SZAs) where the photochemical effect on BrO in the stratosphere is large.

It has to be emphasized that:

- Ozone is produced in the stratosphere mainly in the tropical regions where the Chapman cycle is more effective. Stratospheric ozone is then transported to mid and high latitudes, by the meridional circulation. For non chlorine activated conditions, ozone in the lower stratosphere can be considered (to a certain point) as a tracer due to its long chemical lifetime (typically a month).
- Inorganic bromine is mainly produced in the tropical lower stratosphere by the progressive degradation of organic bromine source gases. As already mentioned, Br_y has a very long chemical lifetime and can be transported to higher latitudes.

Since Br_y and O_3 are both produced in the tropical stratosphere and are sensitive to the dynamic of the atmosphere in a similar way, there is a parallel between Br_y and O_3 which can explain the observed correlation between BrO and O_3 VCDs, if we assume that the bromine partitioning (BrO/Br_y) has weaker spatial variation (see section 4.2.2) than Br_y.
In order to investigate the expected correlation between Br_y and O_3, the BASCOE model has been used. As an example, Fig. 4.3 shows the calculated Br_y VCDs as a function of the corresponding O_3 VCDs for the BASCOE data. The scatter plot displays all model values for grid points within a latitudinal band of 10° around 35°S, for the month of August 2003.

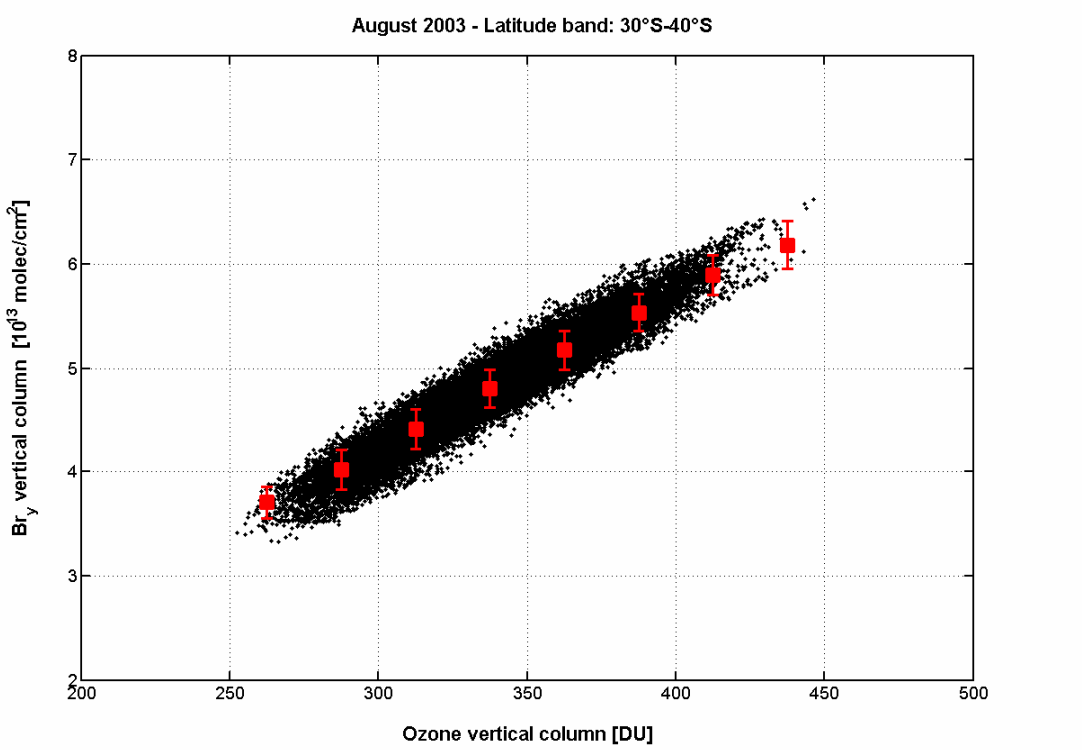

Fig. 4.3: Scatter plot of Br_y and O_3 vertical columns from BASCOE for August 2003 and the latitude band 30°S-40°S. The red squares correspond to the mean Br_y values for O_3 VCD bins of 25 DU.

The red squares correspond to the mean Br_y VCD values (+ standard deviation) whithin O_3 VCD bins of 25 DU. The correlation between Br_y and O_3 is evident on this plot and there is a quasi correspondence between the ozone column and the Br_y column. The scatter plot will change by varying the latitudinal band and month, illustrating the spatial and seasonal variation of the dynamic of the atmosphere.

This noticeable property allows us to build our Br_y profile climatology based only on several inputs:

- Period of the year
- Latitude
- Ozone column

In practice, the advantage of using a parameterization of Br_y profiles based on the total ozone column is that, in addition to the simplicity of the method, the ozone column is a standard product which is retrieved operationally (with an excellent accuracy, less than 1% for moderate SZA) and is easily accessible. Furthermore, the retrieved O_3 column is an effective value, representative for the measured pixel.

The various steps to build the Br_y profiles climatology based on the BASCOE model are:

1. Interpolation of all BASCOE Br_y profiles on a given altitude grid covering the stratosphere
2. Average level-by-level of the Br_y profiles corresponding to each period of the year, latitudinal band and ozone column bins (O_3 VCDs have been calculated beforehand by integrating the BASCOE O_3 profiles). The standard deviation profile is also retained, since it gives an interesting information of the variability of the Br_y profiles.

As an example, Fig. 4.4 presents mean monthly zonal Br_y concentration profiles from the output of the BASCOE model, for March and a latitude band from 40°N to 50°N. The left and right plots correspond to O_3 VCD respectively of 325±12.5 DU and 425±12.5 DU.

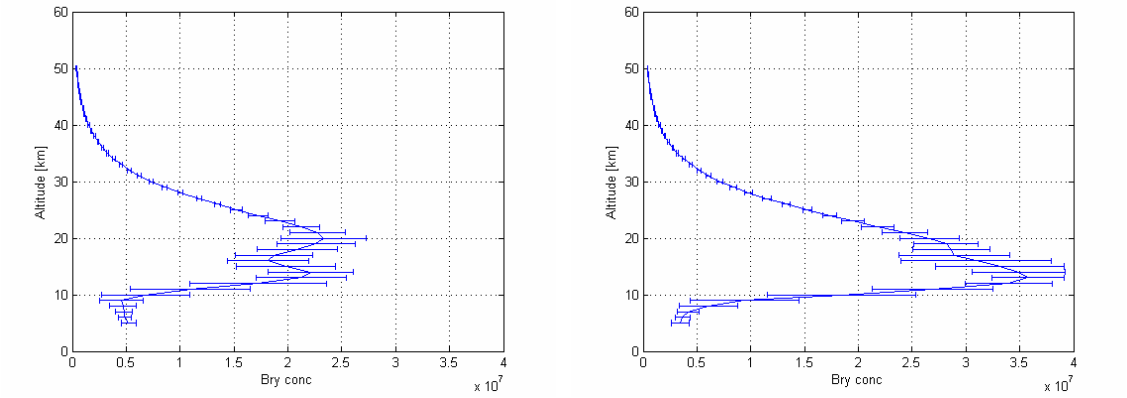

Fig. 4.4: Zonal mean Br_y concentration profiles from the BASCOE model. All modeled Br_y profiles for March and for latitude comprises between 40°N and 50°N have been interpolated on a fixed altitude grid and then averaged level-by-level. The error bars represent the variability of Br_y for each altitude. An additional selection on the model grid points corresponding to O_3 VCD of (left) 325±12.5 DU and (right) 425±12.5 DU has been applied.

It has to be noticed that the two profiles are significantly different only below an altitude of ~25 km. For altitudes between the tropopause (~ 10 km, in this case) and 25 km, the Br_y profile is highly variable due to dynamical effects. However, the selection of the Br_y profiles based on the O_3 VCD results in slight deviations from the mean Br_y profiles. It is good to remember that these profiles only have a physical meaning above the tropopause altitude.

Finally, it has to be pointed out that this approach (based on the correlation between Br_y and O_3) fails for "ozone hole" conditions. Indeed, ozone can no longer be considered as a dynamical tracer since it is rapidly destroyed due to the activation of chlorine species. These particular conditions will be further studied in section 4.2.3.

4.2.2 Photochemical aspects

In this section, the main processes controlling the bromine partitioning (BrO/Br_y) are reviewed and a parameterization of the bromine partitioning is proposed. Here, we restrict ourselves to usual atmospheric conditions. The conditions where the bromine photochemistry is affected by heterogeneous reactions on the surface of PSCs (leading to a denoxification/dehydration of the stratosphere and an eventual activation of chlorine species), is studied in section 4.2.3.

The main photochemical reactions implying bromine compounds in the stratosphere has been presented in section 1.1 and is schematically illustrated in Fig. 1.1. In this work, it is necessary to identify the dominant photochemical reactions as a function of altitude, affecting the bromine partitioning BrO/Br_y (see discussion in Lary et al., 1996a). For this purpose, the BASCOE model is a useful tool, since the profiles of all bromine species (as well as other species like O_3, NO_2, ..) are available for various photochemical conditions. Furthermore, it is also possible to study the diurnal variation of the bromine species as the BASCOE fields are generated for given UT times, so that a diurnal cycle is achieved simply by varying the longitude.

In Fig. 4.5, the BASCOE volume mixing ratio profiles of the most important bromine species in the stratosphere are plotted for typical spring mid-latitude conditions during morning daylight.

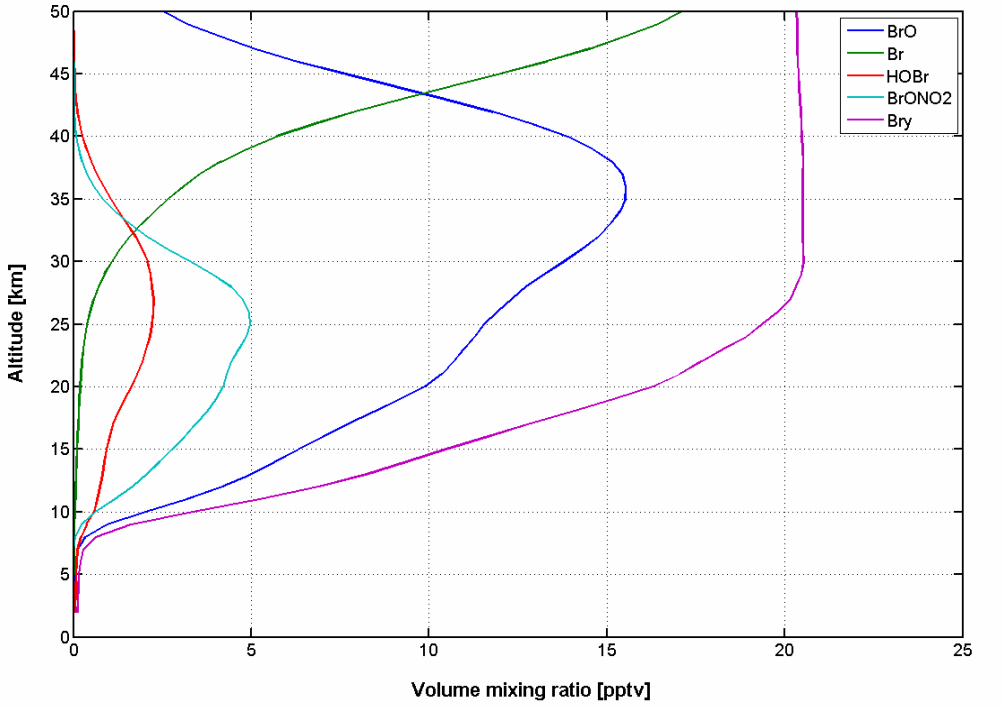

Fig. 4.5: Typical spring mid-latitude volume mixing ratio profiles of BrO, Br, HOBr, $BrONO_2$ and Br_y, for morning conditions.

As expected, the inorganic bromine vmr is close to zero at the tropopause and increases up to ~ 30 km where it reaches a constant value of 22 pptv as all organic bromine compounds have been converted into inorganic forms.
The examination of the profiles of Br, BrO, $BrONO_2$ and HOBr allows us to identify three photochemical regimes:

- From the tropopause to 25 km: BrO is in photochemical equilibrium with its reservoirs ($BrONO_2$ and HOBr) and is the most abundant bromine species. The loss processes of $BrONO_2$ and HOBr are dominated by the photolysis (R11, R12).
- From 25 km to 35 km: the ultraviolet flux is higher and the production of oxygen atom becomes significant. This lead to a progressive conversion of the bromine reservoirs into reactive bromine (Br and BrO). The main loss process of $BrONO_2$ is photolysis (R11), whereas the reaction with O is the main loss of HOBr (R13). Bromine monoxide vmr reaches his maximum around 35 km.
- Above 35 km: the two main reactions are

$$Br + O_3 \rightarrow BrO + O_2 \quad \text{(R1)}$$
$$BrO + O \rightarrow Br + O_2 \quad \text{(R2)}$$

The conversion of BrO into Br is the main loss of BrO in the upper stratosphere and Br becomes the most abundant bromine species above ~ 45 km.

It can be stated that the partitioning of the bromine species in the lower stratosphere depends strongly on the profiles of the reservoir precursors and on the incoming radiation flux as a function of altitude.
In this work, we mainly focus on the stratospheric layer from the tropopause to ~30 km, since the largest contribution to the stratospheric BrO column originates from this layer (see Fig. 4.4). Fig. 4.5 shows that the main bromine reservoir in this altitude region is $BrONO_2$, which is formed by the termolecular reaction $BrO+NO_2+M$ (R6). As a first approximation, the bromine partitioning ratio is:

$$\frac{BrO}{Br_y} \approx \frac{BrO}{BrO + BrONO_2} = \frac{1}{1 + \frac{k_{BrONO_2} NO_2}{J_{BrONO_2}}} \quad (4.2)$$

where k_{BrONO_2} : chemical constant for the formation of $BrONO_2$.

NO_2 : nitrogen dioxide concentration.

J_{BrONO_2} : photodissociation constant of $BrONO_2$.

This relation expresses the balance between the production and the loss (by photodissociation) of $BrONO_2$ which affects directly the bromine partitioning. From equation (4.2), we can deduce that BrO/Br_y is directly controlled by the concentration of NO_2. The chemical constant k_{BrONO_2} varies with altitude through a dependence with the temperature, while the photodissociation constant J_{BrONO_2} varies strongly with altitude and solar zenith angle, but only slightly with the O_3 column (a sensitivity test shows that tripling the O_3 VCD decreases J_{BrONO_2} by 8% maximum, for SZA lower than 90°).

In the upper stratosphere (above 35 km), the bromine partitioning (BrO/Br_y) is essentially controlled by the ratio O/O_3 which is very sensitive to the solar zenith angle.
In summary, the bromine ratio BrO/Br_y profile responds very rapidly to any change in SZA (leading to a diurnal variation of BrO, and of all the other bromine species) and NO_2 concentration profile (BrO will thus have strong latitudinal and seasonal variations).

However, the objective here is to build a simple bromine partitioning climatology for satellite retrieval. A parameterization of BrO/Br_y based on the solar zenith angle and the NO_2 profile is, in that sense, an inconvenient solution, because of the large size of the matrix climatology and the fact that it requires a stratospheric NO_2 profile for each measurement. Therefore, we might be tempted to build a bromine partitioning BrO/Br_y climatology based solely on the:

- Stratosperic NO_2 column
- Solar zenith angle

This practical choice is partly justified by the fact that the stratospheric NO_2 vertical column reflects principally the behavior of the NO_2 concentrations in the lower and middle stratosphere.

At this stage, it is necessary to make several remarks:
◊ The advantage of using the stratospheric NO_2 column is that this information is accessible as an intermediate product in the near-real-time operational retrieval of total and tropospheric NO_2 columns from GOME-2 measurements.
◊ In the following, we will consider only the BASCOE data corresponding to morning conditions, since the GOME-2 instruments have morning overpasses (around 09:30 AM local time at the equator).
◊ The stratospheric NO_2 column is mainly determined by day length (photolysis of the reservoirs) and the solar zenith angle (affecting the diurnal equilibrium NO_2/NO). Therefore, and additional parameterization of BrO/Br_y based on the period of the year and the latitude is redundant.
◊ We will consider here only the data corresponding to SZA lower than 85° in order to avoid the effect of the strong transition of NO_2 at twilight, varying in latitude and time.

This approach is no longer valid for atmospheric conditions where a strong denoxification occurs, since there is no formation of $BrONO_2$ (the main bromine reservoir). This aspect will be treated in more details in section 4.2.3.

4.2.3 Perturbed chemistry conditions

As it has been mentioned before, the parameterization of stratospheric BrO based on the O_3 VCD and stratospheric NO_2 VCD (as dynamical and photochemical tracers respectively) is questionable for ozone hole conditions. Here, we propose a method to reproduce satisfactorily stratospheric BrO profiles for perturbed chemistry conditions. It

has to be pointed out that the solution provided here is only an approximation of the reality. The mechanisms responsible for the formation of the ozone hole are complex and involve dynamical aspects of the stratosphere and heterogeneous chemistry. Diverse non-linear processes are competing, sometimes with typical timescales varying by several orders of magnitude. The main concepts related to polar ozone depletion are well documented (see e.g. Solomon, 1999), and here we intend only to give a brief description of key processes for this study. We focus here on the Antarctic region, where the phenomenon is by far more important than for Arctic region, due to weaker dynamic disturbances.

During winter polar night, the stratosphere is not exposed to sunlight. A strong circumpolar wind (knows as the polar vortex) develops in the polar stratosphere and has the effect to isolate the air over the polar region. Since no light reaches the south pole for several weeks, no photochemistry takes place in the stratosphere and the NO_x species are progressively converted in N_2O_5. Another consequence of the absence of light is that the air temperature within the polar vortex gets very cold. This lead to the formation of particles referred to as Polar Stratospheric Clouds (PSCs). A classification of the PSC types with their composition and formation temperature is presented in Table 4.1.

Table 4.1: PSC classification with respect to their composition and formation temperature.

Type	**Composition**	**Temperature**
PSC 1a	supercooled ternary solution (STS) of $H_2SO_4/H_2O/HNO_3$	< 196 °K
PSC 1b	nitric acid trihydrate (NAT), HNO_3 . 3 H_2O	< 196 °K
PSC 2	pure ice	< 188 °K

Heterogeneous chemical reactions on the surface of PSCs modify considerably the composition of the polar stratosphere. In particular, the conversion of N_2O_5 into nitric acid ($HNO_{3(s)}$) sequestered within the PSCs aerosols is an important phenomenon, called denoxification. The sedimentation of large PSC particles leads to an irreversible removal of considerable amounts of H_2O (dehydration) and HNO_3 (denitrification) from the polar stratosphere. PSCs provide the surface for a number of heterogeneous reactions converting the chlorine reservoir species HCl and $ClONO_2$ to more reactive species as Cl_2 and HOCl. Similar heterogeneous reactions involving bromine species (R 18, R 19, R 20) are also taking place, but are relatively less important since bromine species are present mainly in their reactive forms. At the beginning of the polar spring, the unstable Cl compounds photodissociate rapidly and release Cl atoms (chorine activation). A very effective catalytic mechanism involving Cl, ClO and Cl_2O_2 then occurs, leading to the complete destruction of ozone in few weeks between ~ 15 and 25 km of altitude. The key concept here is that no NO_x is available (due to denoxification and the isolation of air in the polar vortex) to moderate the Cl catalysis. Furthermore, only a small supply of NO_x and O_3 by upper stratospheric layers is expected since the vertical transport is very slow (the vertical wind speed is of about 1 km/month in the polar vortex). Bromine plays an important role during the active photochemistry period through the ClO/BrO cycle which leads to an additional provisioning of reactive Cl and Br atoms (eventually through the intermediate formation of BrCl). In the meantime, the stratosphere becomes warmer at the beginning of polar spring, and the PSCs progressively evaporate starting with PSCs of

type 2. This releases HO_x radicals in the stratosphere and conducts to the partial conversion of Cl into HCl. However, this mechanism occurs after significant ozone loss. In late spring, PSCs of type 1 evaporate, releasing HNO_3 which is photolysed and, at the end, supplied NO_x to the stratosphere. Chlorine nitrate is then formed by the reaction between ClO and NO_2. Progressively, the chlorine reservoirs (HCl and $ClONO_2$) return to their pre-ozone hole levels. The polar vortex in late spring begins to weaken and ozone-rich mid-latitudinal air starts to mix with the low ozone air from the polar vortex. The polar vortex becomes very unstable until its breakup. By summer, the ozone layer has recovered by dynamical mixing of air. Nevertheless, there are large interannual differences of the duration and strength of the ozone hole. This is linked to the year-to-year variations for the persistence and strength of the polar vortex (dynamical aspects), temperature of the stratosphere, PSCs formation and sedimentation rates, halogen loading,..

Here, we intend to investigate the implications of this dynamical and photochemical perturbed regime on stratospheric BrO. As developed in sections 4.2.1 and 4.2.2, we will treat separately the effects on BrO due to the dynamic of the stratosphere and the photochemistry.

1. Dynamics of the stratosphere

As mentioned earlier, a correlation between O_3 and Br_y is expected as long as ozone is not destroyed by fast heterogeneous chemistry. As an illustration, Fig. 4.6 shows the total and partial columns (for 3 layers: below 15 km, between 15 and 19 km, above 19 km) of ozone and inorganic bromine from BASCOE in the southern hemisphere at 00:00 UT for 6 days in 2003 covering a period from early winter to late spring.

(a) 01-07-2003

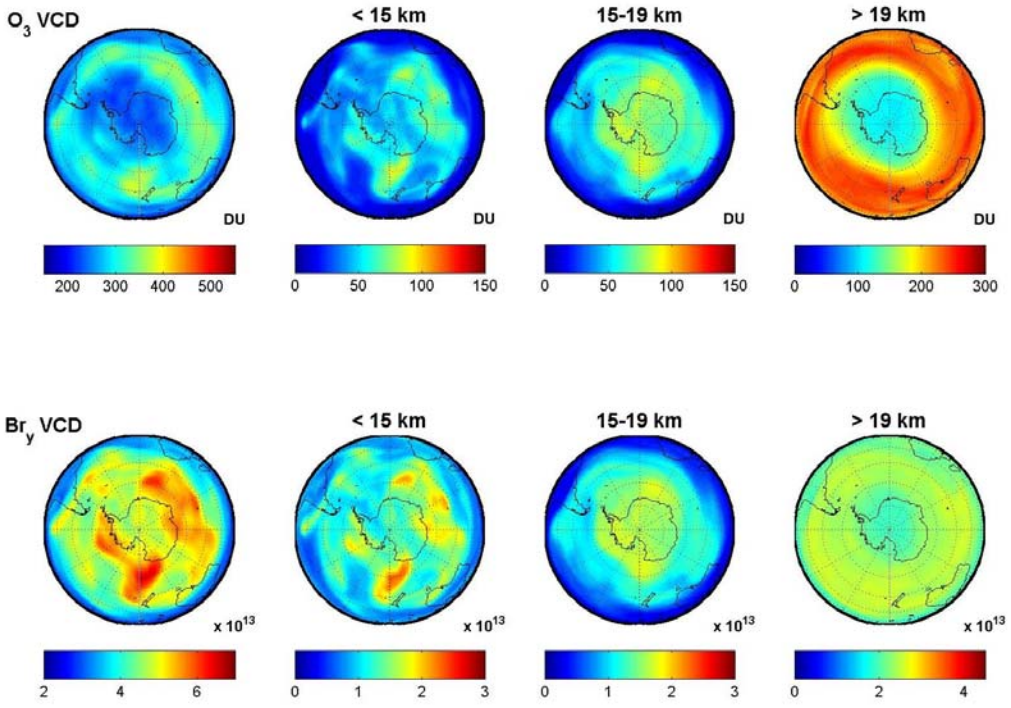

(b) 01-08-2003

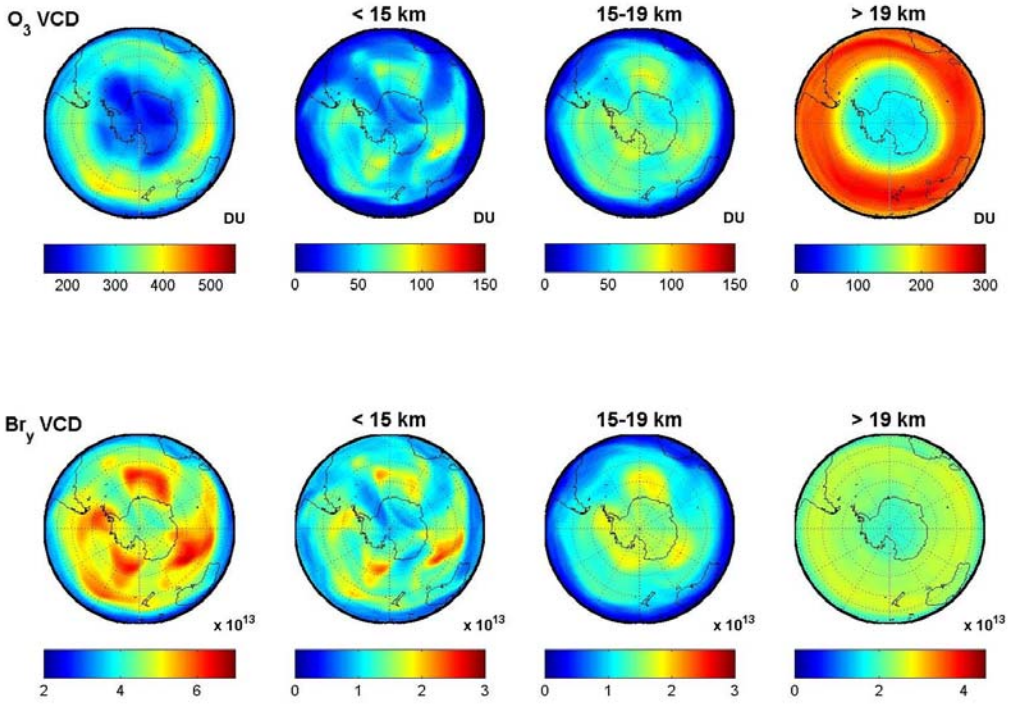

(c) 15-08-2003

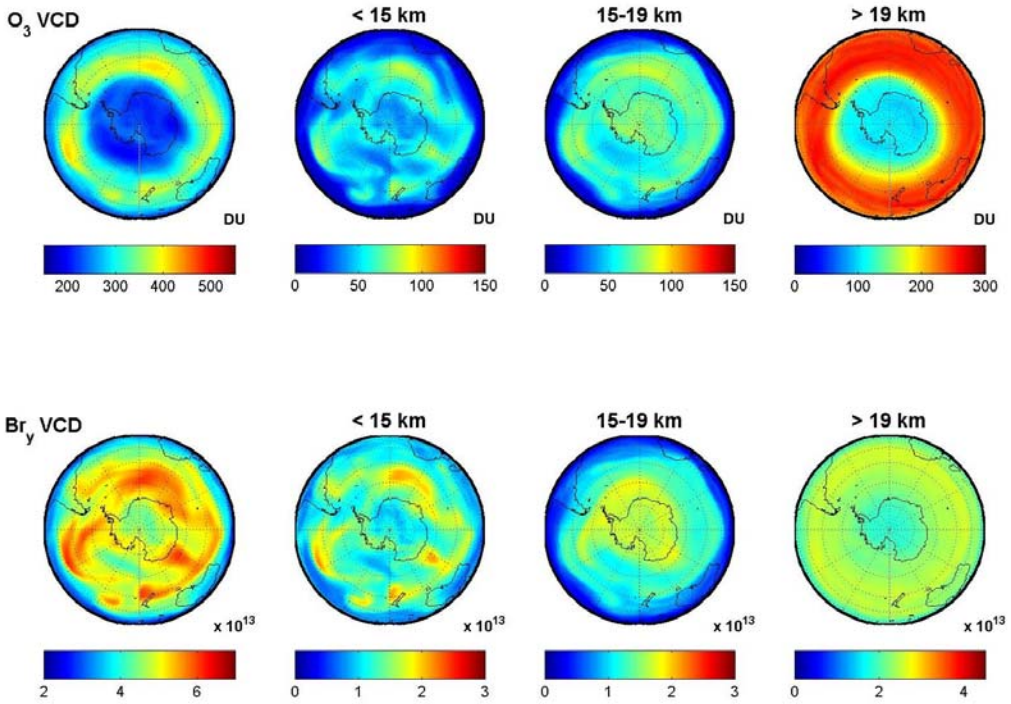

(d) 01-10-2003

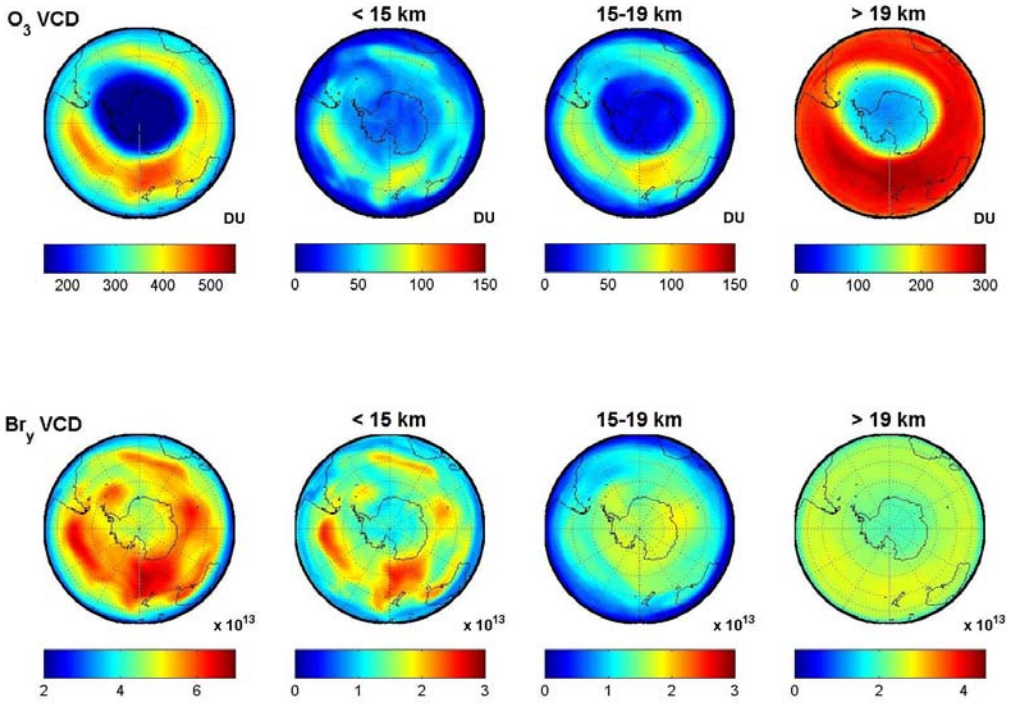

(e) 01-11-2003

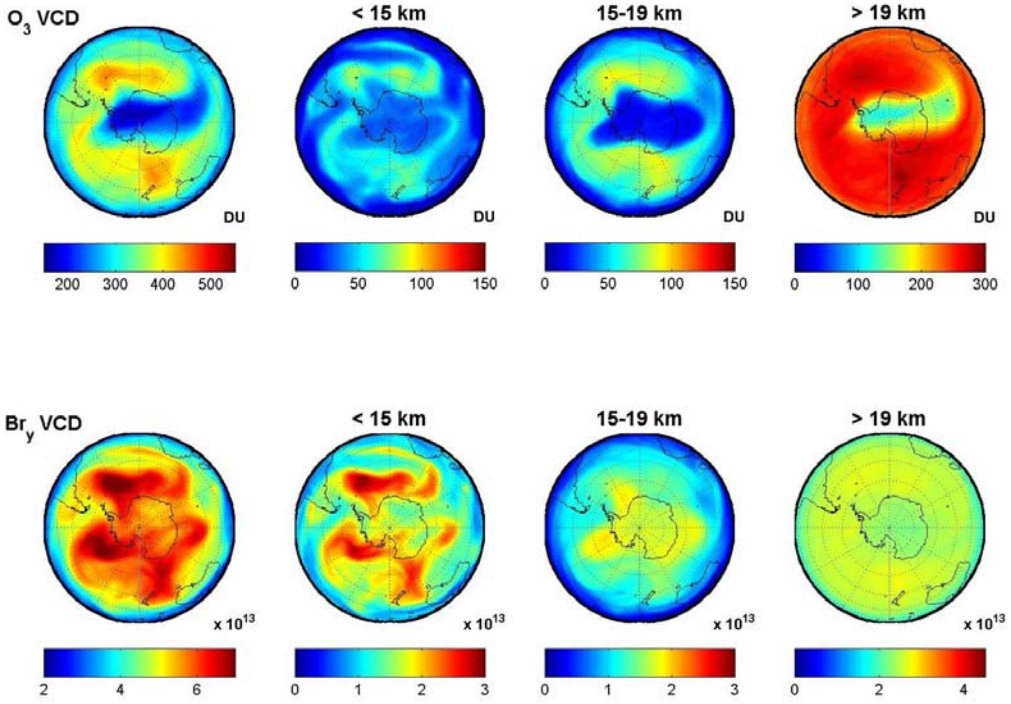

(f) 01-12-2003

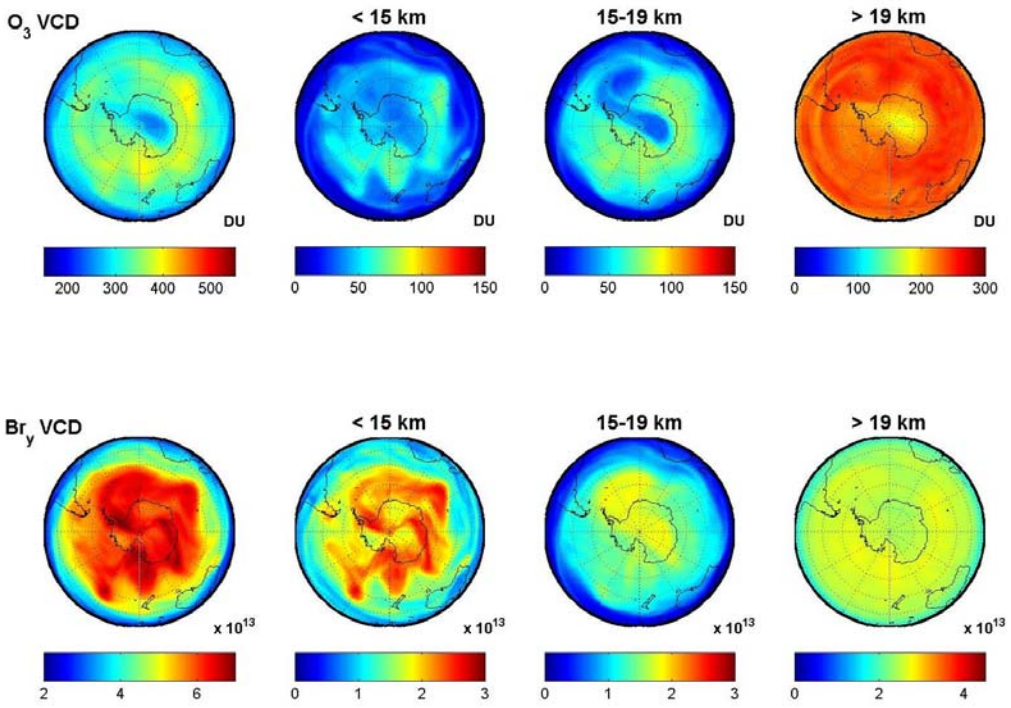

Fig. 4.6: Total and partial columns (below 15 km, between 15 and 19 km, above 19 km) of O_3 (upper plots) and Br_y (lower plots) from BASCOE in the southern hemisphere at 00h00 UT for 6 days in 2003: (a) 01-07, (b) 01-08, (c) 15-08, (d) 01-10, (e) 01-11, (f) 01-12.

- Figure 4.6 (a): In early winter, ozone can still be considered as a dynamical tracer and the correlation between O_3 and Br_y is visible at all latitudes in the "lower" (below 15 km) and "middle" (between 15 and 19 km) layers. In the "upper" layer (above 19 km), low values of ozone are observed at high latitudes. This is due to the meridional stratospheric circulation. In winter, a downward-poleward transport brings poor ozone air parcels in the middle stratosphere leading to lower O_3 vertical columns. The same effect is less visible for Br_y, since inorganic bromine vmr stays constant with altitude above ~ 30 km (22 pptv, see Fig. 4.5). This property emphasizes the necessity to parameterize the Br_y based on the O_3 VCD (to account for the lower stratosphere dynamical structures) and the latitude and time of the year (to account for the evolution of the meridional circulation of the stratosphere).

- Figure 4.6 (b): In late winter, the ozone destruction starts for the polar upper layer. However, the correlations between O_3 and Br_y in the layers below 19 km are still present. Thus, variation of the total ozone VCD within the polar vortex is related to dynamical structures in the lower and middle layers and O_3 VCD can be used, to a certain point, to determine the vertical distribution of Br_y .

- Figure 4.6 (c): In mid-August, the ozone destruction has started in the middle layer on a circle close to the polar vortex edge. It can be seen that the correlation between O_3 and Br_y is less obvious in the middle layer, but is still visible in the lower layer.

- Figure 4.6 (d): In early spring, the ozone destruction concerns the three layers. It is no longer possible to identify correlations between O_3 and Br_y in the polar vortex. Nevertheless, Br_y partial columns show small variations within the vortex.

- Figure 4.6 (e): In mid-spring, the polar vortex weakens and air masses with low ozone and high Br_y amounts (initially in the vortex) will mix with mid-latitude air rich in ozone and with lower levels of Br_y. It is relatively difficult to represent this mixing in a climatology.

- Figure 4.6 (f): In late spring, the ozone hole has almost disappeared.

This suggests that a possible solution to build a general Br_y climatology is to extend the climatology O_3 VCD bin grids to lower values. It is clear from Fig. 4.6 that there will be some limitations to this approach, but the discussion above shows that there is still some information on the Br_y vertical distribution in the O_3 VCD pattern. However, an error study is necessary to determine the suitability of this method. A promising approach also would be to use a parameterization using the O_3 profiles retrieved from the measurements, but it is less convenient.

As a baseline, we propose a generalized Br_y profile climatology dependent on the month of the year, latitude and total ozone columns with the same input grids as for the TOMS v8 ozone profile climatology:

- Month: 1 to 12
- Latitude: 18 latitudinal blocks (10° band) centered around -85°,-75°, … , 85°.
- Total ozone VCD: 10 O_3 VCD blocks (50 DU width) centered around 125, 175, …, 575 DU

In practice, the Br_y profile climatology will be generated by averaging the BASCOE Br_y profiles corresponding to each selection of month, latitude band and ozone VCD band. It has to be noticed that certain values of the climatology will be filled by dummy values for non physical situations (e.g. low O_3 VCD values in spring for northern high-latitudes).

2. Perturbed photochemistry

The bromine photochemistry deviates from the standard regime (essentially controlled by stratospheric NO_2) under denoxification conditions. Since the denoxification occurs in unpolluted regions, the cases of perturbed bromine photochemistry can thus be diagnosed when low NO_2 columns are measured (e.g. lower than ~$1x10^{15}$ molec/cm^2).
Several photochemical scenarios can occur:

◊ denoxification and chlorine activation (~ from August to late September)

In this case, BrO and BrCl are the major inorganic bromine species during daylight.

◊ denoxification and no chlorine activation (October-November)

As the temperature increases, the PSCs of type 2 evaporate and release HO_x species in the stratosphere. Active chlorine is then progressively converted into chlorine reservoirs (mainly HCl). This situation can persist as long as the supply of NO_x species, by the evaporation of PSCs of type 1, is low. Regarding bromine chemistry during morning daylight, this photochemical regime leads to a photochemical equilibrium mainly between BrO, Br and HBr. Indeed, BrCl is no longer an important bromine reservoir and $BrONO_2$ is not significant at sunrise due to the low amount of NO_x for its formation *(R11)* and its conversion into HOBr during the night by heterogeneous reactions *(R18)*. At sunrise, HOBr is rapidly photolysed into Br *(R12)*. The only possible reactions involving Br (see Fig.1.1) are the oxidizing reaction with O_3 *(R1)* to form BrO (followed by the photodissociation to re-form Br *(R3)*) and the reaction with HO_2 *(R9)* to form HBr (followed by the reconversion into Br by reaction with OH *(R16)* or O *(R17)*). HBr constitutes thus the major bromine reservoir for this particular photochemical regime.

These two perturbed photochemical regimes can be differentiated by the amount of active chlorine species in the stratosphere, which is related to the presence or the absence of PSCs. From what has been exposed above, the temperature of the stratosphere (or a related variable) might be used, to a certain point, as an indicator of the photochemical state of the stratosphere.

5 Conclusions and perspectives

In the framework of this Ozone SAF Visiting Scientist project dedicated to BrO column retrieval algorithms for GOME-2, several activities/tasks described in the proposed workplan, have been achieved:

- Optimisation of DOAS settings for BrO retrieval: the consistency between the UPAS DOAS module and the BIRA Windoas code has been checked on sample GOME orbits. An excellent agreement is found, with differences lower than 1-2 %.

- Verification of radiative transfer tools for calculation of box-AMFs: calculations of box-AMFs have been performed for different scenarios (by varying the SZA, the viewing geometry and the ground albedo) using different radiative transfer codes (UVspec/DISORT and LIDORT). The agreement is within 1-2%, except for high VZA at high SZA where the differences are of about 5%. These discrepancies are due to the treatment of the Earth's sphericity, which is different in both models.

- Development of a stratospheric BrO profiles climatology: a new approach for the estimation of the stratospheric BrO content has been developed, based on results of the BASCOE model. The potential of this method to reproduce the important variations of stratospheric BrO is shown to be adequate for the retrieval of tropospheric BrO columns from satellite nadir measurements. The impact of the

atmospheric dynamic on the stratospheric BrO distribution is accounted by using retrieved ozone columns. The effect of photochemistry on stratospheric BrO is determined by considering the stratospheric NO_2 columns. It is also demonstrated that meteorological data as temperature profiles is helpful for the treatment of perturbed photochemical conditions.

In the future, several activities regarding the development of the BrO climatology, are envisaged:

- Validation of BASCOE: Assess the quality of the modeled BrO columns and profiles through comparisons with ground-based and balloon-borne stratospheric BrO observations. Particular attention will be paid to the inorganic bromine budget, through implementation within BASCOE of an up-to-date inventory of organic bromine source gases.
- Improvement of the parameterization of the BrO climatology (particularly for perturbed chemistry conditions). Optimization of the values entries of the climatology look-up-tables. An error analysis is necessary to assess the suitability of the adopted approach and to ensure an accuracy of the BrO columns derived from the climatology of about 10%.
- Investigation of the relevance of establishing a climatology based only on one year of output data. Indeed, on one hand, the austral winter in 2003 is known to be relatively cold, with a deep and long ozone hole. On the other hand, the boreal winter 2003-2004 is characterized by relatively high stratospheric temperatures, leading to almost no event of chlorine activation in the northern hemisphere.
- Generation of the stratospheric BrO climatology.
- Results from the BIRA-IASB GOME BrO residual algorithm, using the new stratospheric BrO climatology as a stratospheric correction, will be compared for consistency to the GOME tropospheric BrO column dataset introduced in section 1.3, on sample orbits.
- Implementation of the stratospheric BrO climatology as part of the GOME-2 operational processor.

Other activities related to the calculation of the tropospheric BrO air mass factors can also be envisaged in the future. The existing surface albedo databases and cloud data sets might be reviewed jointly for suitability in BrO retrieval, especially for polar regions which are of major relevance for BrO. Moreover, different tropospheric BrO profiles representative for the polar “bromine explosion” phenomenon can be tested for tropospheric BrO retrieval improvement.

Acknowledgements

This research has been partly supported by the Belgian Prodex project NOyBry. We wish to thank M.P. Chipperfield (University of Leeds) who provided us with SLIMCAT data.

References

Aliwell, S. R., Van Roozendael, M., Johnston, P.V., Richter, A., Wagner, T., et al.: Analysis for BrO in zenith-sky spectra: An intercomparison exercise for analysis improvement, J. Geophys. Res., 107, D140, doi: 10.1029/2001JD000329, 2002.

Bobrowski, N., Höninger, G., Galle, B., and Platt, U.: Detection of bromine monoxide in a volcanic plume, Nature, 423, 273-276, 2003.

Bruns, M., Bovensmann, H., Richter, A., and Burrows, J.P.: A stratospheric BrO climatology for the GOME-2 instruments, O3-SAF Visiting Scientist, final report, 2003.

Burrows, J.P., Richter, A., Dehn, A., Deters, B., Himmelmann, S., Voigt, S., and Orphal, J.: Atmospheric remote-sensing reference data from GOME: Part 1. Temperature-dependent absorption cross section of NO_2 in the 231-794 nm range, JQSRT, 60, 1025, 1998.

Burrows, J.P., Richter, A., Dehn, A., Deters, B., Himmelmann, S., et al: Atmospheric remote sensing reference data from GOME: Part 2. Temperature dependent absorption cross section of O_3 in the 231-794 nm range, JQSRT, 61, 509-517, 1999.

Cantrell, Davidson, McDaniel, Shetter and Calvert, Temperature-Dependent Formaldehyde Cross Sections in the Near-Ultraviolet Spectral Region, J. Phys. Chem., 94, 3902-3908, 1990.

Chance, K.: Analysis of BrO measurements from the Global Ozone Monitoring Experiment, Geophys. Res. Lett., 25, 3335-3338, 1998.

Chipperfield M. P., Khattatov, B. V., and Lary, D. J.: Sequential assimilation of stratospheric chemical observations in a three-dimensional model, J. Geophys. Res., 107 (D21), 4585, doi:10.1029/2002JD002110, 2002.

Daerden, F., Larsen, N., Chabrillat, S., Errera, Q., Bonjean, S., Fonteyn, D., Hoppel, K., and Fromm, M. : A 3D-CTM with detailed online PSC-microphysics : analysis of the Antarctic winter 2003 by comparison with satellite observations, Atmos. Chem. Phys. Discuss., 6, 8511-8552, 2006.

Dorf, M.: Investigation of inorganic stratospheric bromine using balloon-borne DOAS measurements and model simulations, PhD. Thesis, University of Heidelberg, Germany, 2005.

Dorf, M., Bösch, H., Butz, A., Camy-Peyret, C., Chipperfield, M., Engel, A., Goutail,F., Grunow, K., Hendrick, F., Hrechanyy, S., Naujokat, B., Pommereau, J.-P., Van Roozendael, M., Sioris, C., Stroh, F., Weidner, F., and Pfeilsticker, K.: Balloon-borne

stratospheric BrO measurements: Intercomparisons with ENVISAT/SCIAMACHY BrO limb profiles, Atmos. Chem. Phys., 6, 2483-2501, 2006.

Errera, Q. and Fonteyn, D.: Four-dimensional variational chemical assimilation of CRISTA stratospheric measurements, J. Geophys. Res., 106, 12253-12265, 2001.

Fitzenberg, R., Bösch, R., Camy-Peyret, C., Chipperfiel, M.P.,Harder, H., Platt, U., Sinnhuber, B.-M., Wagner, T., and Pfeilsticker, K.: First profile measurements of tropospheric BrO, Geophys. Res. Lett., 27, 2921-2924, 2000.

Frieβ, U., Hollwedel, J., König-Langlo, Wagner, T., and Platt, U.: Dynamics and chemistry of tropospheric bromine explosion events in the Antarctic coastal region, J. Geophys. Res., 109, D06305, doi:10.1029/2003JD004133, 2004.

Geer, A.J., Lahoz, W.A., Bekki, S., Bormann, N., Errera, Q., Eskes, H.J., Fonteyn, D., Jackson, D.R., Juckes, M.N., Massart, S., Peuch, V.-H., Rharmili, S., and Segers, A.: The ASSET intercomparison of ozone analysis: method and first results, Atmos. Chem. Phys., 6, 5445-5474, 2006.

Greenblatt, G.D., Orlando, J.J., Burkholder, J.B., and Ravishankara, A.R.: Absorption measurements of oxygen between 330 and 1140 nm, J. Geophys. Res., 95, 18577-18582, 1990.

Gür, B., Spietz, P., Orphal, J., and Burrows, J. P.: Absorption Spectra Measurements with the GOME-2 FMs using the IUP/IFE-UB's Calibration Apparatus for Trace Gas Absorption Spectroscopy CATGAS, Final Report, ESA/EUMETSAT Contract No. 16007/02/NL/SF, October 2005.

Hausmann, M., and Platt, U.: Spectroscopic measurement of bromine oxide and ozone in the high Arctic during Polar Sunrise Experiment 1992, J. Geophys. Res., 99, 25399-25414, 1994.

Hebestreit, K., Stutz, J., Rosen, D., Matveiv, V., Peleg, M., Luria, M., and Platt, U.: DOAS measurements of tropospheric bromine oxide in mid-latitudes, Science, 283, 55-57, 1999.

Hönninger, G., and Platt, U.: Observations of BrO and its vertical distribution during surface ozone depletion at Alert, Atmos. Environ., 36, 2481-2489, 2002.

Koelemeijer, R. B. A.: Surface reflectivity spectra derived from GOME data.

Koelemeijer, R. B. A., Stamnes, P., Hovenier, J.W., de Haan, J.F.: A fast method for retrieval of clouds parameters using oxygen A band measurements from the Global Ozone Monitoring Experiment , J. Geophys. Res., 106(D4), 3475-3490, 10.1029/2000JD900657, 2001.

Kreher, K., Johnston, P.V., Wood, S.W., Nardi, B., and Platt, U.: Ground-based measurements of tropospheric and stratospheric BrO at Arrival Heights, Antartica, Geophys. Res. Lett., 24, 3021-3024, 1997.

Kromminga, H., Orphal, J., Voigt, S., and Burrows, J. P., Fourier-transform-spectroscopy of symmetric chlorine dioxide (OClO), Proc. EC Advanced Study Course (ASTAIRE 1999), Bergen, Norway, 1999.

Larsen, N.: Polar Stratospheric Clouds. Microphysical and optical models, Scientific report 00-06, Danish Meteorological Institute, available from http://www.dmi.dk/, 2000.

Lary, D.J.: Gas phase atmospheric bromine photochemistry, J. Geophys. Res., 101, pp1505-1516, 1996a.

Lary, D.J., Chipperfield, M.P., Toumi, R. and Lenton, T.: Heterogeneous atmospheric bromine photochemistry, J. Geophys. Res., 101, pp1489-1504, 1996b.

Leser, H., Höninger, G., and Platt, U.: Max-DOAS measurements of BrO and NO_2 in the marine boundary layer, Geophys. Res. Lett., 30, 1537, doi:10.1029/2002GL015811, 2003.

Mayer, B. and Kylling, A.: Technical note: The libRadtran software package for radiative transfer calculations – description and examples of use, Atmos. Chem. Phys., 5, 1855-1877, 2005.

Palmer, P.I., Jacob, D.J., Chance, K., Martin, R.V.,Spurr, R.J.D., Kurosu, T.P., Bey, I., Fiore, A., and Li, Q. : Air mass factor formulation for spectroscopic measurements from satellites: Application to formaldehyde retrievals from the Global Ozone Monitoring Experiment, J. Geophys. Res., 106, 14539-14550, 2001.

Pundt, I., Van Roozendael, M., Wagner, T., Richter, A., Chipperfield, M., Burrows, J. P., Fayt, C., Hendrick, F., Pfeilsticker, K., Platt, U., and Pommereau, J.-P.: Simultaneous UV-vis measurementsof BrO from balloon, satellite and ground: implications for tropospheric BrO, in Proc. Fifth European Symp. on polar stratospheric ozone 1999. Air Poll. Res. Report 73, EUR 19340, European Commission, Brussels, Belgium, edited by N. R.P. Harris, M. Guirlet, and G.T. Amanatidis, pp. 316-319, 2000.

Pundt, I., Pommereau, J.-P., Chipperfield, M.P., Van Roozendael, M., and Goutail, F.: Climatology of the stratospheric BrO vertical distribution by balloon-borne UV-visible spectrometry, J. Geophys. Res., 107(D24), 4806, doi:10.1029/2002JD002230, 2002.

Reichler, T., Dameris, M., and Sausen, R.: Determining the tropopause height from gridded data , Geophysical Res. Letters, Vol. 30, No. 20, 2042, 2003.

Richter, A., Wittrock, F., Eisinger, M., and Burrows, J. P.: GOME observations of tropospheric BrO in Northern Hemispheric spring and summer 1997, Geophys. Res. Lett., 25, 2683-2686, 1998.

Richter, A., Wittrock, F., Ladstätter-Weissenmayer, A., and Burrows, J. P.: GOME measurements of stratospheric and tropospheric BrO , Adv. Space Res., 29, 1667-1672, 2002a.

Richter, A., and Burrows, J.P.: Tropospheric NO_2 from GOME measurements, Adv. Space Res., 29, 1673-1683, 2002b.

Sander, S.P., Friedl, R. R., Golden, D. M., Kurylo, M.J., Huie, R.E., Orkin, V.L., Moortgaat, G.K., Ravishankara, A.R., Kolb, C.E., and Molina, M.J.: Chemical Kinetics and Photochemical Data for Use in Atmospheric Studies. Evaluation Number 14, Publication 00-3, JPL, 2003.

Salawitch, R.J., Weisenstein, D.K., Kovalenko, L.J., Sioris, C.E., Wennberg, P.O., Chance, K., Ko, M.K.W., and McLinden, C.A.: Sensitivity of ozone to bromine in the lower stratosphere, Geophys. Res. Lett.,32, L05811, doi: 10.1029/2004GL021504, 2005.

Salawitch R.J., Atmospheric chemistry: biogenic bromine, Nature, 439, 275-277, 2006.

Schofield, R., Kreher, K., Connor, B.J., Johnston, P.V., Thomas, A., Shooter, D., Chipperfield, M.P., Rodgers, C.D., and Mount, G.H.: Retrieved tropospheric and stratospheric BrO columns over Lauder, New Zealand., J. Geophys. Res., 109, D14304, doi:10.1029/2003JD004463, 2004.

Siddans, R. et al.: Analysis of GOME-2 Slit function measurements, Final Report, EUMETSAT Contract No. EUM/CO/04/1298/RM, 2006.

Sinnhuber, B.-M., Arlander, D. W., Bovensmann, H., et al.: Comparison of measurements and model calculations of stratospheric bromine monoxide, J. Geophys. Res., 107 (D19), 4398, doi:10.1029//2001JD000940, 2002.

Sinnhuber, B.-M., Rozanov, A., Sheode, N., Afe, O.T., Richter, A., Sinnhuber, M., Wittrock, F., and Burrows, J.P.: Global observations of stratospheric bromine monoxide from SCIAMACHY, Geophys. Res. Lett., 32, L20810, doi: 10.1029/2005GL023839, 2005.

Sioris, C. E., Kovalenko, L.J., McLinden, C.A., Salawitch, R.J., Van Roozendael, M., Goutail, F., Dorf, M., Pfeilsticker, K., Chance, K., von Savigny, C., Liu, X., Kurosu, T.P., Pommereau, J.-P., Bösch, H., and Frerick, J.: Latitudinal and vertical distribution of bromine monoxide in the lower stratosphere from Scanning Imaging Absorption Spectrometer for Atomspheric Chartography limb scattering measurements, J. Geophys. Res., 111, D14301, doi:10.1029/2005JD006479, 2006.

Solomon, S.: Stratospheric ozone depletion: a review of concepts and history, Reviews of Geophysics, Vol. 37, 275-316, 1999.

Spurr, R.J.D., Kurosu, T.P., and Chance, K.V.: A linearized discrete ordinate radiative transfer model for atmospheric remote sensing retrieval, J. Quant. Spectrosc. Radiat. Transfer, 68, 689-735, 2001

Spurr, R.J.D, LIDORT V2PLUS: A comprehensive radiative transfer package for nadir viewing spectrometers, remote sensing of clouds and atmosphere, Proc. SPIE Int. Soc. Opt., 3750, 2003.

Theys, N., De Smedt, I., Van Roozendael. M., Fayt, C., Chipperfield, M., Post, P., Van der A, R.: Total and tropospheric BrO derived from GOME and SCIAMACHY as part of the TEMIS project, in Proc. Envisat/ERS Symposium, Salzburg, 6-10 September, 2004.

Theys, N., Hendrick, F., Van Roozendael, M., De Smedt, I., Fayt, C., Van der A, R.: Retrieval of BrO columns from SCIAMACHY and their validation using ground- based DOAS measurements, in Proceeding Atmospheric Science Conference, ESRIN, Frascati, Italy, 8-12 May 2006.

Theys, N., Van Roozendael, M., Hendrick, F., Fayt, C., Hermans, C., De Mazière, M. (2007): Retrieval of stratospheric and tropospheric BrO columns from multi-axis DOAS measurements at Reunion Island, to be submitted to Atmospheric Chemistry and Physics.

Van Roozendael, M., C. Fayt, J.-C. Lambert, I. Pundt, T. Wagner, A. Richter, and K. Chance, Development of a bromine oxide product from GOME, in Proc. ESAMS'99-European Symposium on Atmospheric Measurements from Space, ESTEC, Noordwijk, The Netherlands, 18-22 January 1999, ESA WPP-161, p. 543-547, 1999.

Van Roozendael, M., Wagner, T., Richter, A., Pundt, I., Arlander, D., Burrows, J. P., Chipperfield, M., Fayt, C., Johnston, P. V., Lambert, J.-C., Kreher, K., Pfeilsticker, K., Platt, U., Pommereau, J.-P., Sinnhuber, B.-M., Tornkvist, K. K., and Wittrock, F.: Intercomparison of BrO measurements from ERS-2 GOME, ground-based and balloon platforms , Adv. Space Res., 29, 1661-1666, 2002.

Vigouroux, C., De Mazière, M., Errera, Q., Chabrillat, S., Mahieu, E., Duchatelet, P., Wood, S., Smale, D., Mikuteit, S., Blumenstock, T., Hase, F., and Jones, N.: Comparisons between ground-based FTIR and MIPAS N_2O and HNO_3 profiles before and after assimilation in BASCOE, Atmos. Chem. Phys., 7, 377-396, 2007.

von Glasow, R., von Kuhlmann, R., Lawrence, M. G., Platt, U., and Crutzen P.J.: Impact of reactive bromine chemistry in the troposphere, Atmos. Chem. Phys. Discuss.,4, 4877-4913, 2004.

Vountas, M., Rozanov, V.V., and Burrows, J.P., Ring effect: Impact of Rotational Raman Scattering on Radiative Transfer in Earth's Atmosphere, JQSRT, 60, 943, 1998.

Wagner, T., and Platt, U.: Satellite mapping of enhanced BrO concentrations in the troposphere, Nature, 395, 486-490, 1998.

Wagner, T., Leue, C., Wenig, M., Pfeilsticker, K., and Platt, U.: Spatial and temporal distribution of enhanced boundary layer BrO concentrations measured by the GOME instrument aboard ERS-2, J. Geophys. Res., 106, 24225-24235, 2001.

Wilmouth, D. M., Hanisco, T.F. , Donahue, N. M., and Anderson, J.G.: Fourier transform ultraviolet spectroscopy of the $A(^2\Pi_{3/2}) \leftarrow X(^2\Pi_{3/2})$ transition of BrO, J. Phys. Chem, 103, 8935-8944, 1998.